

ANALYSIS OF THE SCHWARZ DOMAIN DECOMPOSITION METHOD FOR THE CONDUCTOR-LIKE SCREENING CONTINUUM MODEL

ARNOLD REUSKEN AND BENJAMIN STAMM

Abstract. We study the Schwarz overlapping domain decomposition method applied to the Poisson problem on a special family of domains, which by construction consist of a union of a large number of fixed-size subdomains. These domains are motivated by applications in computational chemistry where the subdomains consist of van der Waals balls. As is usual in the theory of domain decomposition methods, the rate of convergence of the Schwarz method is related to a stable subspace decomposition. We derive such a stable decomposition for this family of domains and analyze how the stability “constant” depends on relevant geometric properties of the domain. For this, we introduce new descriptors that are used to formalize the geometry for the family of domains. We show how, for an increasing number of subdomains, the rate of convergence of the Schwarz method depends on specific local geometry descriptors and on one global geometry descriptor. The analysis also naturally provides lower bounds in terms of the descriptors for the smallest eigenvalue of the Laplace eigenvalue problem for this family of domains.

1. Introduction. In this article, we analyze scaling properties of the Schwarz overlapping domain decomposition method for the Poisson problem: find $u \in H_0^1(\Omega^M)$ such that

$$-\Delta u = f, \quad \text{in } H^{-1}(\Omega^M) := (H_0^1(\Omega^M))'.$$

Here $\Omega^M \subset \mathbb{R}^3$ is a bounded Lipschitz domain and $H_0^1(\Omega^M)$ denotes the usual Sobolev space of functions with weak derivatives in $L^2(\Omega^M)$ with vanishing Dirichlet-trace. We investigate the behavior of the Schwarz iterative method when Ω^M consists of a increasing number $M = 2, 3, \dots$ of *fixed-size* overlapping subdomains $\{\Omega_i\}_{i=1}^M$. We are particularly interested in the case that the subdomains Ω_i are overlapping balls with comparable radii.

The motivation for studying this problem comes from numerical simulations in computational chemistry. Recently, a domain decomposition method has been proposed [1, 16, 18, 19, 22] in the context of so-called implicit solvation models, more precisely for the COnductor-like Screening MOdel (COSMO) [14] which is a particular type of continuum solvation model (CSM). In a nutshell, such models account for the mutual polarization between a solvent, described by an infinite continuum, and a charge distribution of a given solute molecule of interest. It therefore takes the long-range polarization response of the environment (solvent) into account. We refer to the review articles [17, 24] for a thorough introduction to continuum solvation models.

While for most of the applications of domain decomposition methods, the computational domain remains fixed (such as in engineering-like applications) and finer and finer meshes are considered, applications in the present context deal with different molecules consisting of a (very) large number of atoms. Each atom is associated with a corresponding van der Waals (vdW)-ball with a given and element-specific radius so that the total computational domain consists of the union of those vdW-balls. For a set of different molecules the computational domain is therefore changing and the Schwarz domain decomposition exhibits different convergence properties. For example, for an (artificial) linear chain of atoms of increasing length the Schwarz domain decomposition is scalable and does not require a so-called coarse space correction [1].

A general convergence analysis of the Schwarz domain decomposition iterative method for the *family* of domains Ω^M , $M = 2, 3, \dots$, can not easily be deduced from

classical analyses of domain decomposition methods available in the literature, e.g. [8, 25, 26]. This is due to the fact that these classical analyses assume a *fixed domain* that is decomposed in an increasing number of (overlapping) subdomains of decreasing size, whereas in the setting outlined above the subdomains all have a given comparable size and the *global domain changes* when the number of subdomains is increased. It turns out that for a convergence analysis in the latter case it is not obvious how results and tools available in classical analyses can be applied. Therefore, in recent papers [2, 3, 4, 5, 6] this topic has been addressed and new results on the convergence of the Schwarz domain decomposition iterative method on a family of domains Ω^M , $M = 2, 3, \dots$, were obtained. More precisely, the first theoretical results were obtained for a chain to rectangles in two dimensions [2, 3], which were later generalized to chain-like structures of disks and balls in two respectively three dimensions [4, 5]. These results, however, cover only (very) special cases as each of the subdomains has a nonempty intersection with the boundary of the computational domain Ω^M , i.e. no balls are allowed that are contained inside Ω^M . A first step towards a more general analysis can be found in [6], which analyzes how the error propagates and contracts in the maximum norm in a general geometry. It is shown that for a molecule with N -layers, it takes $N + 1$ iterations until the first contraction in the maximum norm is obtained. This is essential to understand the contraction mechanism, in particular for the first iterations, but unfortunately does not provide much insight on the rate of (asymptotic) convergence.

In this paper we present a general analysis which covers many cases that occur in applications and that goes beyond the previously mentioned contributions. Although the presentation is somewhat technical, due to the fact that we have to formalize the geometry of the family of domains Ω^M , $M = 2, 3, \dots$, the convergence analysis is based on a few fundamental ingredients known from the field of subspace correction methods and Sobolev spaces, which are combined with new descriptors of the geometries considered. We outline the main components of the analysis. We use the well-established framework of subspace correction methods [26]. In [27], for the successive (also called “multiplicative”) variant of the Schwarz domain decomposition method a convergence analysis in a general Hilbert space setting is derived. The contraction number of the error propagation operator (in the natural energy norm) can be expressed in only *one stability parameter* (s_0 in Lemma 2.1 below). This parameter quantifies the *stability of the space decomposition*. We bound this stability parameter by introducing a *new variant of the pointwise Hardy inequality*. This variant allows estimates that take certain important global geometry properties into account. Using this we derive, for example, a uniform bound in M , if we have a chain like family of domains, and a bound that grows (in a specified way) as a function of M , if we have a family of “globular” domains. It is well-known from the literature on domain decomposition methods that in the latter case one should use an additional “global coarse level space”. We propose such a space for our setting and analyze the rate of convergence of the Schwarz method that includes this additional coarse space.

The paper is organized as follows. In Section 2 the Schwarz domain decomposition that we analyze in this paper is explained and an important result on the rate of convergence of this method, known from the literature, is given. This result essentially states that the contraction number (in the energy norm) of the Schwarz method is characterized by only *one* quantity, which controls the stability of the space decomposition. In Section 3 we introduce new descriptors of the specific class of domains (union of overlapping balls) that is relevant for our applications. Furthermore, for this

class of domains a natural partition of unity is defined and analyzed. This partition of unity is used in Section 4 to derive bounds for the stability quantity. A further key ingredient in our analysis of the Schwarz method is a variant of the pointwise Hardy inequality, that is also presented in Section 4. A main result of the paper is given Theorem 4.8. As is well-known from the theory of Schwarz domain decomposition methods, in certain situations the efficiency of such a method can be significantly improved by using a global (coarse level) space. For our particular application this issue is studied in Section 5. Finally, in Section 6 we present results of numerical experiments, which illustrate certain properties of the Schwarz domain decomposition method and relate these to the results of the convergence analysis.

2. Problem formulation and Schwarz domain decomposition method.

We first describe the class of domains Ω^M that we consider. Let $m_i \in \mathbb{R}^3$, $i = 1, \dots, M$, be the centers of balls and R_i the corresponding radii. We define

$$\begin{aligned}\Omega_i &:= B(m_i; R_i) = \{x \in \mathbb{R}^3 \mid \|x - m_i\| < R_i\}, \\ \Omega^M &:= \cup_{i=1}^M \Omega_i.\end{aligned}$$

We consider the Poisson equation: determine $u \in H_0^1(\Omega^M)$ such that

$$a(u, v) := \int_{\Omega^M} \nabla u \cdot \nabla v \, dx = f(v) \quad \text{for all } v \in H_0^1(\Omega^M), \quad (2.1)$$

with a given source term $f \in H^{-1}(\Omega^M)$. For a subdomain $\omega \subset \Omega_M$ we denote the Sobolev seminorm of first derivatives by $|v|_{1,\omega}^2 := \int_{\omega} \|\nabla v(x)\|^2 \, dx$. For solving this problem we use the Schwarz domain decomposition method, also called successive subspace correction in the framework of Xu and Zikatanov [27]. This method is as follows:

Let $u^0 \in H_0^1(\Omega^M)$ be given.

for $\ell = 1, 2, \dots$

$$u_0^{\ell-1} := u^{\ell-1}$$

for $i = 1 : M$

Let $e_i \in H_0^1(\Omega_i)$ solve

$$a(e_i, v_i) = f(v_i) - a(u_{i-1}^{\ell-1}, v_i) \quad \text{for all } v_i \in H_0^1(\Omega_i). \quad (2.2)$$

$$u_i^{\ell-1} := u_{i-1}^{\ell-1} + e_i$$

endfor

$$u^\ell := u_M^{\ell-1}$$

endfor

This is a linear iterative method and its error propagation operator is denoted by E . We then obtain

$$u - u^\ell = E(u - u^{\ell-1}) = \dots = E^\ell(u - u^0).$$

An analysis of this method is presented in an abstract Hilbert space framework in [27]. Here we consider only the case, in which the subspace problems in (2.2) are solved *exactly*.

REMARK 2.1. There also is an additive variant of this subspace correction method (called “parallel supspace correction” in [27]). This method may be of interest because it has much better parallelization properties. This additive variant can be analyzed with tools very similar to the successive one given above. We further discuss this in Remark 5.2.

As norm on $H_0^1(\Omega^M)$ it is convenient to use $|v|_{1,\Omega^M}^2 := a(v, v)$. In this norm the bilinear form $a(\cdot, \cdot)$ has ellipticity and continuity constants both equal to 1. The corresponding operator norm on $H_0^1(\Omega^M)$ is also denoted by $|\cdot|_{1,\Omega^M}$. On $H^1(\Omega_i)$ we use the seminorm $|v_i|_{1,\Omega_i}^2 := a(v_i, v_i)$, $v_i \in H^1(\Omega_i)$. We need the following projection operator $P_i : H_0^1(\Omega^M) \rightarrow H_0^1(\Omega_i)$ defined by

$$a(P_i v, w_i) = a(v, w_i) \quad \text{for all } w_i \in H_0^1(\Omega_i).$$

We recall an important result from [27] (Corollary 4.3 in [27]).

LEMMA 2.1. *Assume that $\sum_{i=1}^M H_0^1(\Omega_i)$ is closed in $H_0^1(\Omega^M)$. Define*

$$s_0 := \sup_{\substack{v \in H_0^1(\Omega^M) \\ |v|_{1,\Omega^M} = 1}} \inf_{\sum_{j=1}^M v_j = v} \sum_{i=1}^M \left| P_i \sum_{j=i+1}^M v_j \right|_{1,\Omega_i}^2, \quad (2.3)$$

where $v_j \in H_0^1(\Omega_j)$ for all j . Then

$$|E|_{1,\Omega^M}^2 = \frac{s_0}{1 + s_0} \quad (2.4)$$

holds.

The constant s_0 quantifies the *stability of the decomposition* of the space $H_0^1(\Omega^M)$ into the sum of subspaces $H_0^1(\Omega_i)$. Due to the result (2.4) we have that the contraction number of the Schwarz domain decomposition method (in the natural $|\cdot|_{1,\Omega^M}$ norm) depends only on s_0 . Hence, if s_0 is independent of certain parameters (e.g., in our setting M) then the contraction rate is also robust w.r.t. these parameters. In the remainder of this paper we analyze this stability quantity s_0 depending on the geometrical setting and the closedness assumption needed in Lemma 2.1. The analysis is based on a particular decomposition $v = \sum_{i=1}^M \theta_i v = \sum_{i=1}^M v_i$ with $v_i := \theta_i v$ and $(\theta_i)_{1 \leq i \leq M}$ forms a partition of unity that is introduced and analyzed in the next section.

3. Geometric properties of the domain Ω^M and partition of unity. The number M of balls is arbitrary and in the analysis below it is important that in estimates and in further results we explicitly address the dependence on the number M . The estimates in the analysis below depend on certain geometry related quantities that we introduce in this section.

In order to formalize the geometry dependence in our estimates, we introduce a (infinite but countable) family of geometries $\{\mathcal{F}_M\}_M$ indexed by the increasing number $M \in \mathbb{N}$ of balls, where each element $\mathcal{F}_M = \{B(m_i, R_i) \mid i = 1, \dots, M\}$ represents the set of balls defining the geometry Ω^M characterized by the set of centers and radii. We further introduce

$$R_{\min}(\mathcal{F}_M) := \min_{1 \leq i \leq M} R_i, \quad R_{\max}(\mathcal{F}_M) := \max_{1 \leq i \leq M} R_i.$$

We first start with stating basic assumptions on the geometric structure of the considered domains.

ASSUMPTION 3.1 (Geometry assumptions).

- (A1) For each M , we assume that Ω^M is connected. This assumption is made without loss of generality. If Ω^M has multiple components, the problem (2.1) decouples into independent problems on each of these components and the analysis presented below applies to the problem on each component.
- (A2) For each M , we assume that there are no i, j , with $i \neq j$, such that $\Omega_i \subset \Omega_j$, i.e., balls are not completely contained in larger ones. Otherwise, the inner balls can be removed from the geometric description without further consequences.
- (A3) We assume the radii of the balls to be uniformly bounded in the family $\{\mathcal{F}_M\}_M$: there exists R_{\max}^∞ and $R_{\min}^\infty > 0$ such that

$$\sup_M R_{\max}(\mathcal{F}_M) \leq R_{\max}^\infty < \infty, \quad \inf_M R_{\min}(\mathcal{F}_M) \geq R_{\min}^\infty > 0.$$

- (A4) (Exterior cone condition) We assume that for each $y \in \partial\Omega^M$ there exists a circular cone $C(y)$ with aperture $2\beta \geq 2\beta^M > 0$, apex y and axis $n(y)$ that belongs entirely to the outside of Ω^M in a neighborhood of y , i.e., $B(y; \epsilon) \cap C(y) \cap \Omega^M = \emptyset$ for $\epsilon > 0$ sufficiently small. We furthermore assume that β^M is uniformly bounded from below: there exists $\beta^\infty > 0$ such that

$$\inf_M \beta^M \geq \beta^\infty > 0.$$

Related to this we have the following result.

LEMMA 3.1. *For $y \in \partial\Omega^M$ denote by i_t , $t = 1, \dots, r$, all indices such that $y \in \partial\Omega_{i_t}$, and define $v_t = \frac{m_{i_t} - y}{\|m_{i_t} - y\|}$. Assumption (A4) is equivalent to the following one:*

There exists $\gamma_\alpha^\infty > 0$ such that for each M and for each $y \in \partial\Omega^M$, there exists a unit vector $n(y)$ such that $-n(y) \cdot v_t \geq \gamma_\alpha^\infty > 0$ for all $t = 1, \dots, r$. This implies that all vectors v_t are situated on one side of the plane that is perpendicular to $n(y)$ and passing through y .

Proof. The limiting aperture of a cone with apex y in the direction of $n(y)$ is given by twice the minimal angle of $n(y)$ with the tangential plane at y to each ball Ω_{i_t} , $t = 1, \dots, r$. This angle is illustrated by $\beta_{i_t}(y)$ in Figure 3.1. Note that $\alpha_{i_t} + \beta_{i_t} = \frac{1}{2}\pi$, where α_{i_t} is the angle between $n(y)$ and v_{i_t} . Hence β_{i_t} is bounded away from zero if and only if α_{i_t} is bounded away from $\frac{1}{2}\pi$, i.e. $\cos(\alpha_{i_t})$ bounded away from zero. Finally note that $\cos(\alpha_{i_t}) = -n(y) \cdot v_{i_t}$, which shows that the uniform boundedness away from zero of the interior cone angles β_{i_t} and of $-n(y) \cdot v_{i_t}$ are equivalent conditions. \square

The condition of Lemma 3.1 provides a precise mathematical statement in terms of geometrical notions. This condition for instance excludes the following scenarios, using the notation $D = \dim(\text{span}(v_{i_1}, \dots, v_{i_r}))$, and where Figure 3.1 (middle and right) provides a schematic illustration of those two cases:

$D = 1$: Intersection of two balls $\bar{\Omega}_{i_t}$ is only one point, that is, y and the centers m_{i_t} are on one line. In turn, only the plane \mathcal{P} passing through y which is perpendicular to line passing through v_{i_1} and v_{i_2} does not intersect Ω^M locally around y and there exists no cone of positive aperture with apex y that (locally) belongs to the outside of Ω^M .

$D = 2$: Intersection of three balls $\bar{\Omega}_{i_t}$ is one point. Here, only the line $y + tw$, with $w \in \mathbb{R}^3$ being the normal vector to the plane passing through $v_{i_1}, v_{i_2}, v_{i_3}$ and

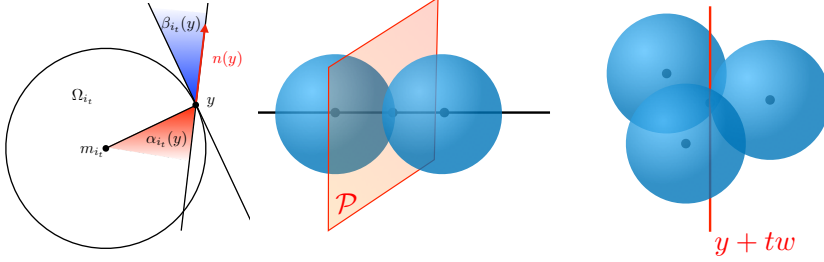


FIG. 3.1. Relation between α and β (left), illustrative example for the case $D = 1$ (middle) and for the case $D = 2$ (right) related to the violation of condition **(A4)**.

$t \in (-\varepsilon, \varepsilon)$, belongs to the outside of Ω^M . In turn, there exists no cone of positive aperture with apex y that (locally) belongs to the outside of Ω^M .

3.1. Local geometry indicators. We introduce certain geometry descriptors, which we call *indicators*, that are related to the specific geometry of the domain Ω^M and that will be used in the estimates derived below. We will distinguish between local and global indicators, the former only being dependent on *local geometrical features* whereas the latter being dependent on the *global topology* of the geometric configuration.

We introduce some further definitions. We take a fixed $\mathcal{F}_M \in \{\mathcal{F}_M\}_M$, with corresponding domain Ω^M . We decompose the index set $\mathcal{I} := \{1, \dots, M\}$ into two disjoint sets by introducing $\mathcal{I}_{\text{int}} := \{i \in \mathcal{I} \mid \partial\Omega_i \cap \partial\Omega^M = \emptyset\}$ (“interior balls”) and $\mathcal{I}_{\text{b}} := \mathcal{I} \setminus \mathcal{I}_{\text{int}}$ (“boundary balls”). The corresponding (overlapping) subdomains are denoted by $\Omega_{\text{int}} := \cup_{i \in \mathcal{I}_{\text{int}}} \Omega_i$, $\Omega_{\text{b}} := \cup_{i \in \mathcal{I}_{\text{b}}} \Omega_i$. It may be that \mathcal{I}_{int} is an empty set. We define, for $i \in \mathcal{I}$, $\mathcal{N}_i := \{j \in \mathcal{I} \mid \Omega_i \cap \Omega_j \neq \emptyset\}$, $\mathcal{N}_i^0 := \mathcal{N}_i \setminus \{i\}$. For $i \in \mathcal{I}_{\text{b}}$ we define $\Gamma_i := \partial\Omega_i \cap \partial\Omega^M$. Further, define

$$\begin{aligned} \delta_i(x) &:= \max\{0, R_i - \|x - m_i\|\}, & x \in \overline{\Omega}^M, \quad i \in \mathcal{I}, \\ \delta(x) &:= \sum_{i \in \mathcal{I}} \delta_i(x), & x \in \overline{\Omega}^M. \end{aligned}$$

Hence, on Ω_i the function δ_i is the distance function to $\partial\Omega_i$, which is extended by 0 outside Ω_i . Note that $\delta(x) = \sum_{j \in \mathcal{N}_i} \delta_j(x)$ for $x \in \Omega_i$ and that, for any $x \in \Omega^M$, there holds that $\delta(x) = 0$ if and only if $x \in \partial\Omega^M$.

In the following, we list the indicators that are used in the upcoming analysis.

INDICATOR 3.1 (Maximal number of neighbors). Define

$$N_{\max} := \max_{i \in \mathcal{I}} \text{card}(\mathcal{N}_i). \quad (3.1)$$

i.e., $N_{\max} - 1$ is the maximal number of neighboring balls that overlap any given ball Ω_i . Note, that if to each Ω_i we associate a number $\alpha_i \geq 0$, then $\sum_{i=1}^M \sum_{j \in \mathcal{N}_i} \alpha_j \leq N_{\max} \sum_{i=1}^M \alpha_i$ holds.

INDICATOR 3.2 (Maximal overlap indicator). Let N_0 be the smallest integer such that:

$$\max_{x \in \Omega^M} \text{card}\{j \mid x \in \Omega_j\} \leq N_0. \quad (3.2)$$

Hence, $N_0 - 1$ is the maximal number of neighboring balls that overlap any given point $x \in \Omega_i$ of any given ball Ω_i .

Note that for $i \in \mathcal{I}_{\text{int}}$ we have $\partial\Omega_i \subset \cup_{j \in \mathcal{N}_i^0} \Omega_j$, hence $\delta(x) > 0$ for all $x \in \partial\Omega_i$, and thus $\delta(x) > 0$ for all $x \in \Omega_i$. In the same vein, we recall that for all $x \in \Omega^M$ such that $\text{dist}(x, \partial\Omega^M) > 0$, there holds $\delta(x) > 0$. This motivates us to define the following indicator.

INDICATOR 3.3 (Stable overlap indicator). We define

$$\gamma_{\text{int}} := \min_{x \in \Omega_{\text{int}, \beta}} \delta(x) > 0, \quad (3.3)$$

where

$$\Omega_{\text{int}, \beta} := \{x \in \Omega^M \mid x \in \Omega_{\text{int}} \text{ or } \text{dist}(x, \partial\Omega^M) > R_{\min}^\infty \sin(\beta^\infty)\}. \quad (3.4)$$

With this definition, there holds

$$\delta(x) \geq \gamma_{\text{int}}, \quad (3.5)$$

for all $x \in \Omega_{\text{int}}$ or such that $\text{dist}(x, \partial\Omega^M) > R_{\min}^\infty \sin(\beta^\infty)$. Note that by construction, this is a local indicator.

REMARK 3.1. The indicator γ_{int} is a measure for the amount of overlap between any interior ball and its neighboring balls. The indicator is small if there exists a point $x \in \Omega_i$, with $i \in \mathcal{I}_{\text{int}}$, that is simultaneously close to $\partial\Omega_i$ and to the boundary $\partial\Omega_j$ of all balls Ω_j with $x \in \Omega_j$.

A proof of the following lemma, giving rise to a further indicator, is given in Appendix 8.1.

LEMMA 3.2 (Stable overlap for boundary balls). *Under Assumption (A4), there exists $\gamma_b > 0$, such that*

$$\delta(x) \geq \gamma_b \text{dist}(x, \partial\Omega^M) \quad \text{for all } x \in \Omega_b. \quad (3.6)$$

INDICATOR 3.4 (Stable overlap for boundary balls). *The constant $\gamma_b > 0$ defined in Lemma 3.2 is considered as a geometry indicator.*

The indicator γ_b employed in (3.6) clearly is a local one. An explicit formula $\gamma_b = \gamma_b(R_{\min}, R_{\max}, \beta^\infty)$ is given in Eqn. (8.4).

The four indicators introduced above are all natural ones, which are directly related to the number of neighboring balls and the size of the overlap between neighboring balls.

We need one further local indicator, which needs some introduction. In the analysis of the Schwarz method we use a (natural) partition of unity, cf. Section 3.3. The gradient of some of these partition of unity functions is unbounded at $\partial\Omega^M$, where their growth behaves like $x \rightarrow (\text{dist}(x, \partial\Omega^M))^{-1}$. To be able to handle this singular behavior, we need an integral Hardy estimate of the form

$$\left(\int_{\Omega_b} \left(\frac{u(x)}{\text{dist}(x, \partial\Omega^M)} \right)^2 dx \right)^{\frac{1}{2}} \leq c |u|_{1, \Omega^M} \quad \text{for all } u \in H_0^1(\Omega^M),$$

cf. Corollary 4.2. One established technique to derive such an estimate is as in e.g. [11, 13], where *pointwise* Hardy estimates are used to derive integral Hardy

estimates. The analysis in this approach is based on a certain “fatness assumption” for the complement of the domain $\Omega^{M,c} := \mathbb{R}^3 \setminus \Omega^M$. Here we follow this approach and below we will introduce a local indicator that quantifies this exterior fatness of the domain, which is very similar to the fatness indicator used in [11, 13] (cf., for example, Proposition 1 in [11]). Before we define the fatness indicator, note that due to the definition of Ω^M as a union of balls and assumption **(A4)**, we have the following property

$$\forall y \in \partial\Omega^M : \exists r_0 > 0, c > 0 : |B(y; r) \cap \Omega^{M,c}| \geq c|B(y; r)| \quad \forall r \in (0, r_0]. \quad (3.7)$$

INDICATOR 3.5 (Local exterior fatness indicator). For $i \in \mathcal{I}_b$ and $x \in \Omega_i$ we define a closest point projection on Γ_i by $p(x)$, i.e., $p(x) \in \Gamma_i$ and $\|p(x) - x\| = \text{dist}(x, \Gamma_i)$. From (3.7) it follows that there exists $\hat{c}_i > 0$ (depending on the constants $c = c(y)$ in (3.7) and possibly also on R_i) such that

$$|B(p(x); \|p(x) - x\|) \cap \Omega^{M,c}| \geq \hat{c}_i |B(p(x), \|p(x) - x\|)|, \quad \text{for all } x \in \Omega_i, \quad (3.8)$$

with $\Omega^{M,c} := \mathbb{R}^3 \setminus \Omega^M$. We define

$$\gamma_f := \min_{i \in \mathcal{I}_b} \hat{c}_i > 0. \quad (3.9)$$

REMARK 3.2. We call this a *local* exterior fatness indicator because \hat{c}_i depends only on a small neighbourhood of Ω_i , consisting of points that have distance at most R_i to Ω_i . The quantity \hat{c}_i essentially (only) depends on two geometric parameters related to exterior cones with apex at $y \in (\partial\Omega_i \cap \partial\Omega^M)$, namely the maximum possible aperture and the maximal cone height such that the cone is completely contained in $\Omega^{M,c}$. For points lying only on one sphere $\partial\Omega_i$, the cone can be chosen to be as wide as a flat plane. For points lying on an intersection arc $\partial\Omega_i \cap \partial\Omega_j$, the largest aperture of the cone is determined only by the center and radii of the two balls Ω_i, Ω_j . Finally any point lying on an intersecting point of three or more boundary spheres can be assigned a cone whose maximal aperture depends on the radii and centers of the associated balls. Figure 3.2 (left) provides a schematic illustration. The maximal cone height at $y \in (\partial\Omega_i \cap \partial\Omega^M)$ is related to the width of $\Omega^{M,c}$ at y in the direction of the axes of the cone, see also Figure 3.2 (right) for a schematic 2D-illustration. If these apertures and heights are bounded away from zero (uniformly in $y \in (\partial\Omega_i \cap \partial\Omega^M)$), the quantity \hat{c}_i is bounded away from zero. In our applications we consider domains Ω^M such that the apertures and heights satisfy this property.

The set of *local geometry indicators* is denoted by

$$\mathcal{G}_L^M := \{N_{\max}, N_0, \gamma_{\text{int}}^{-1}, \gamma_b^{-1}, \gamma_f^{-1}\}. \quad (3.10)$$

We emphasize that \mathcal{G}_L^M depends only on *local geometry properties* of the domain (as explained above) and does not depend on the global topology of Ω^M (e.g., not relevant whether Ω^M is a linear chain of balls or has a globular form for example). We thus assume the following assumption.

ASSUMPTION 3.2 (Asymptotic geometry assumption).

(A5) We assume that the local geometry indicators \mathcal{G}_L^M are uniformly bounded in the family $\{\mathcal{F}_M\}_M$.

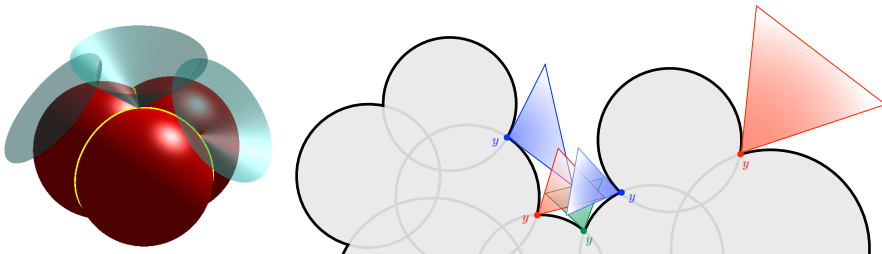


FIG. 3.2. Inserting cones of maximal aperture at the boundary points (left). Illustration of some inserted cones in the definition of the global fatness property (right).

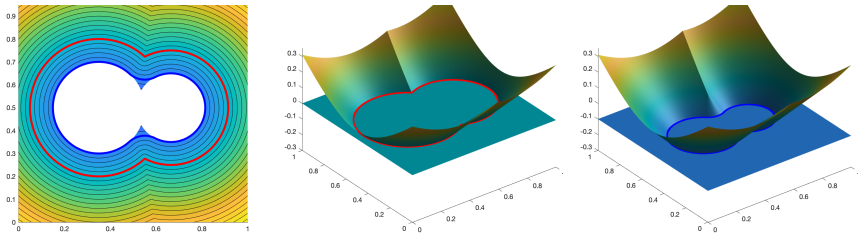


FIG. 3.3. Illustration of the signed distance function to the SAS and its level sets that define the SAS (red) and the SES (blue). The original domain Ω^M is illustrated in white. The distance between the two isolines is the so-called “probe radius”.

3.2. Global geometry indicator. In the analysis below we need a Poincaré-Friedrichs inequality $\|u\|_{L^2(\Omega^M)} \leq c|u|_{1,\Omega^M}$ for $u \in H_0^1(\Omega^M)$, cf. Lemma 4.7. As is well-known, the constant c in this inequality depends on *global* geometry properties of the domain Ω^M and is directly related to the smallest Laplace eigenvalue in $H_0^1(\Omega^M)$. To control this constant we use an approach, presented in Section 4.1 below, based on pointwise Hardy estimates. For this approach to work one needs a measure for “global exterior fatness”. This measure resembles the one used in Indicator 3.5, but there are two important differences. Firstly, we now consider $x \in \Omega^M$ instead of only $x \in \Omega_b$. Secondly, for $x \in \Omega^M$, instead of the corresponding closest point projection $p(x)$ (used in Indicator 3.5) we now take a possibly different exterior point $b(x) \in \Omega^{M,c} = \mathbb{R}^3 \setminus \Omega^M$ such that with $d(x) := \|x - b(x)\|$ the exterior volume $|B(b(x); d(x)) \cap \Omega^{M,c}|$ is comparable to the volume $|B(b(x); d(x))|$. The latter property is a key ingredient in the derivation of satisfactory pointwise Hardy estimates. It turns out that taking $b(x) = p(x)$ is not satisfactory. Below, we present a construction of “reasonable” points $b(x)$ that is adapted to the special class of domains that we consider, namely a union of balls. In the field of applications that we consider, this domain corresponds to a “solute molecule” that is surrounded by “solvent molecules”. In this setting the so-called Solvent Accessible Surface (SAS) of the solute molecule (Ω^M) is defined by the center of a ball (“an idealized spherical probe”) rolling over the solute molecule, that is, the surface enclosing the region in which the center of the ball can not enter. The Solvent Excluded Surface (SES), defined by the same spherical probe, is the surface enclosing the region that can be accessed by this spherical probe [15, 21, 7]. Below in our construction we use these SAS-SES notions which are very natural for our class of domains. Explanations and further properties can be found in [20]. Here we give only a few definitions and properties that are relevant for our analysis.

For a given (probe) radius $r_p > 0$ the precise definition of the SAS is as follows. We introduce

$$\begin{aligned}\Omega_{i,\text{sas}}(r_p) &:= B(m_i; R_i + r_p) = \{x \in \mathbb{R}^3 \mid \|x - m_i\| < R_i + r_p\} \\ \Omega_{\text{sas}}^M(r_p) &:= \cup_{i=1}^M \Omega_{i,\text{sas}}(r_p),\end{aligned}$$

and define $\text{SAS} := \text{SAS}(r_p) := \partial\Omega_{\text{sas}}^M(r_p)$. Let f_{sas} be the signed distance function to SAS (positive in Ω_{sas}^M), hence, $\text{SAS} = f_{\text{sas}}^{-1}(0)$. We define

$$\text{SES} := \text{SES}(r_p) := f_{\text{sas}}^{-1}(r_p) \subset \Omega^{M,c}.$$

We refer to Figure 3.3 for a graphical illustration of the definition of the SES and the SAS. Further, we denote the maximal distance to the $\partial\Omega^M$ by

$$d_{\Omega^M} := \max_{x \in \Omega^M} \text{dist}(x, \partial\Omega^M).$$

A property of the SAS-SES construction is that the balls with center on $\text{SAS}(r_p)$ and radius r_p (these are tangent to $\text{SES}(r_p)$) are completely contained in $\Omega^{M,c}$. We will use these balls in the construction of balls $B(b(x); d(x))$, $x \in \Omega^M$, $b(x) \in \Omega^{M,c}$, $d(x) := \|x - b(x)\|$ that have ‘‘sufficient exterior volume’’. To determine a suitable r_p we use $r_p = \lambda d_{\Omega^M}$, with $\lambda > 0$ a parameter that will be specified below. We now explain this construction. A closest point projection on $\text{SES}_\lambda := \text{SES}(\lambda d_{\Omega^M})$ and the corresponding distance are denoted by

$$b_\lambda(x) \in \arg \min_{y \in \text{SES}_\lambda} \|x - y\|, \quad d_\lambda(x) := \|b_\lambda(x) - x\|, \quad x \in \Omega^M.$$

The maximum distance to SES_λ is denoted by $d_{\text{SES}}(\lambda) := \max_{x \in \Omega^M} d_\lambda(x)$. Note that the following properties hold

$$\begin{aligned}\lim_{\lambda \rightarrow 0^+} d_\lambda(x) &= \text{dist}(x, \partial\Omega^M), & \lim_{\lambda \rightarrow \infty} d_\lambda(x) &= \text{dist}(x, \partial\text{conv}(\Omega^M)), \\ \lim_{\lambda \rightarrow 0^+} d_{\text{SES}}(\lambda) &= d_{\Omega^M}, & \lim_{\lambda \rightarrow \infty} d_{\text{SES}}(\lambda) &= \max_{x \in \Omega^M} \text{dist}(x, \partial\text{conv}(\Omega^M)).\end{aligned}\tag{3.11}$$

Define for all $x \in \Omega^M$, $B_0(x) := B(\hat{b}(x); \hat{r}(x))$, with $\hat{r}(x) := \min(\lambda d_{\Omega^M}, \frac{1}{2}d_\lambda(x))$ and $\hat{b}(x) := b_\lambda(x) + \hat{r}(x) \frac{b_\lambda(x) - x}{\|b_\lambda(x) - x\|}$.

First, note that by the construction of the SES_λ , there holds $B(\hat{p}(x); \lambda d_{\Omega^M}) \subset \Omega^{M,c}$, with $\hat{p}(x) := b_\lambda(x) + \lambda d_{\Omega^M} \frac{b_\lambda(x) - x}{\|b_\lambda(x) - x\|}$, i.e. this corresponds to the definition of the SES of ‘‘rolling a ball with radius $r_p = \lambda d_{\Omega^M}$ and center on the SAS’’. The point $\hat{p}(x) \in \text{SAS}$ denotes this center of the ball. See Figure 3.4 for an illustration and [20] for further explanations. Since $\hat{r}(x) \leq \lambda d_{\Omega^M}$, there holds that for all $z \in B_0(x)$

$$\|z - \hat{p}(x)\| \leq \|z - \hat{b}(x)\| + \|\hat{b}(x) - \hat{p}(x)\| < \hat{r}(x) + (\lambda d_{\Omega^M} - \hat{r}(x)) = \lambda d_{\Omega^M},$$

and thus

$$B_0(x) \subset B(\hat{p}(x); \lambda d_{\Omega^M}) \subset \Omega^{M,c}.$$

Second, for any $z \in B_0(x)$, there holds

$$\|z - b_\lambda(x)\| \leq \|z - \hat{b}(x)\| + \|\hat{b}(x) - b_\lambda(x)\| < 2\hat{r}(x) \leq d_\lambda(x),$$

and thus

$$B_0(x) \subset B(b_\lambda(x); d_\lambda(x)) =: B(x).$$

Hence, for $x \in \Omega^M$ we have

$$\frac{|B(x)|}{|B_0(x)|} = \frac{d_\lambda(x)^3}{\hat{r}(x)^3} = 8 \max \left\{ \left(\frac{d_\lambda(x)}{2\lambda d_{\Omega^M}} \right)^3, 1 \right\} \leq 8 \max \left\{ \left(\frac{d_{\text{SES}}(\lambda)}{2\lambda d_{\Omega^M}} \right)^3, 1 \right\}.$$

We define

$$\gamma_\lambda = \frac{1}{8} \min \left\{ \left(\frac{2\lambda d_{\Omega^M}}{d_{\text{SES}}(\lambda)} \right)^3, 1 \right\}, \quad (3.12)$$

and thus the exterior fatness estimate $|B_0(x)| \geq \gamma_\lambda |B(x)|$ for all $x \in \Omega^M$ holds. In the Hardy estimates used below (cf. (4.3)) we are interested in (possibly small) bounds of the quotient $d_{\text{SES}}(\lambda)/\gamma_\lambda$. This motivates the introduction of the following indicator:

INDICATOR 3.6 (Global exterior fatness indicator). *Assume that*

$$\lambda_{\min} := \arg \min_{\lambda > 0} \frac{d_{\text{SES}}(\lambda)}{\gamma_\lambda} \quad (3.13)$$

exists, cf. Remark 3.3. Define the corresponding global fatness indicator

$$d_F := \frac{d_{\text{SES}}(\lambda_{\min})}{\gamma_F}, \quad \text{with } \gamma_F := \gamma_{\lambda_{\min}}. \quad (3.14)$$

It follows that for any $x \in \Omega^M$, there exists a corresponding point $b(x) \in \Omega^{M,c}$ such that

$$|B(b(x); \|b(x) - x\|) \cap \Omega^{M,c}| \geq \gamma_F |B(b(x); \|b(x) - x\|)|. \quad (3.15)$$

REMARK 3.3. The function $\lambda \rightarrow q(\lambda) := \frac{d_{\text{SES}}(\lambda)}{\gamma_\lambda}$ in (3.13) is not necessarily continuous. Discontinuities can appear, for example, for λ values at which holes in $\Omega_{\text{sas}}^M(\lambda d_{\Omega^M})$ “disappear”. In the generic case, however, a (possibly non-unique) minimizer λ_{\min} as in (3.13) exists. If this is not the case, we choose a λ_{\min} value such that d_F as in (3.14) is close to $\inf_{\lambda > 0} \frac{d_{\text{SES}}(\lambda)}{\gamma_\lambda} > 0$.

In the literature, e.g. [13], a property as in (3.15) is called a uniform (exterior) fatness property of the corresponding domain, and this notion is related to that of variational 2-capacity, hence the name that we have chosen. We continue with a short discussion of this global indicator.

1) It is clear from its definition that d_F is a global indicator and that it has the following upper and lower bounds

$$\begin{aligned} d_F &\geq 8d_{\Omega^M} = 8 \max_{x \in \Omega^M} \text{dist}(x, \partial\Omega^M), \\ d_F &\leq \lim_{\lambda \rightarrow \infty} \frac{d_{\text{SES}}(\lambda)}{\gamma_\lambda} = 8 \max_{x \in \Omega^M} \text{dist}(x, \partial\text{conv}(\Omega^M)). \end{aligned}$$

The quantity d_F can be seen as a measure for the globularity of the domain Ω^M that involves the maximal distance to a SES ($d_{\text{SES}}(\lambda_{\min})$) and the maximal distance to the boundary $\partial\Omega^M$ (d_{Ω^M}).

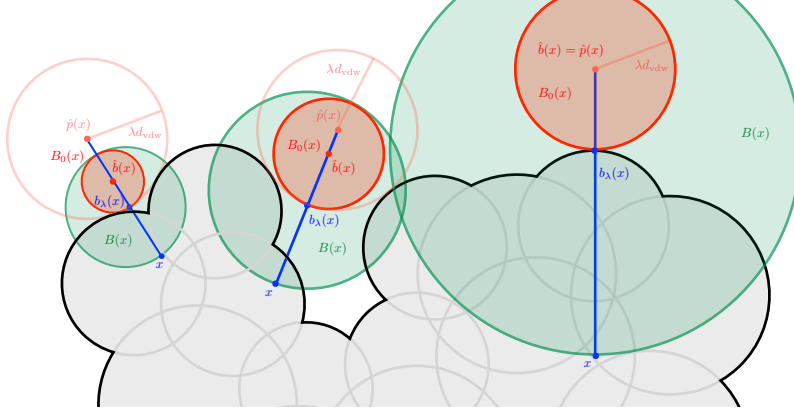


FIG. 3.4. Illustration of the geometrical setup to define the global fatness property.

- 2) In the particular case where Ω^M consists of a linear chain of overlapping uniform balls, with radius R , of length M , we have $d_{\Omega^M} = R$, $d_{\text{SES}}(\lambda) = R$, and thus $d_F = 8R$, i.e., d_F is independent of M . On the other hand, when considering a geometry of uniform balls whose centers lie on the unit grid $[1, L]^3$ with radius $= R > \sqrt{3}$ (in order that no inner holes appear), we obtain $d_{\Omega^M} = d_{\text{SES}}(\lambda) = \frac{1}{2}(L - 1) + R$, hence, $d_F = 4(L - 1) + 8R$. In this case d_F is proportional to $L = M^{1/3}$ as L increases.
- 3) Another consequence of the construction above is that the entire cavity Ω^M can be covered by balls $B(y; R_y)$ with centers y on the $\text{SES}_{\lambda_{\min}} = \text{SES}(\lambda_{\min} d_{\Omega^M}) \subset \Omega^{M,c}$, radii $R_y \leq d_{\text{SES}}(\lambda_{\min})$ and each of these balls contains a smaller ball of radius $\min\{\lambda_{\min} d_{\Omega^M}, \frac{1}{2} R_y\}$ that lies entirely in $\Omega^{M,c}$.

3.3. Partition of unity. In this section we introduce a (natural) partition of unity, based on the local distance functions δ_i , $i \in \mathcal{I}$, and derive smoothness properties for the elements in this partition of unity. In the bounds for derivatives that are proven below only local geometry indicators from \mathcal{G}_L^M are involved.

Note that since δ_i is the distance function to the boundary in Ω_i we have

$$\|\nabla \delta_i(x)\| = 1, \quad x \in \Omega_i, \quad \|\nabla \delta_i(x)\| = 0, \quad x \notin \bar{\Omega}_i, \quad (3.16)$$

One easily checks that $\delta(x) = \sum_{i=1}^M \delta_i = 0$ if and only if $x \in \partial\Omega^M$. We further define

$$\theta_i(x) := \frac{\delta_i(x)}{\delta(x)}, \quad x \in \Omega^M.$$

The system $(\theta_i)_{1 \leq i \leq M}$ forms a partition of unity (PU) of Ω^M subordinate to the cover $(\Omega_i)_{1 \leq i \leq M}$:

$$\begin{aligned} 0 \leq \theta_i \leq 1 \quad (1 \leq i \leq M) \quad \text{on } \Omega^M, \\ \sum_{i=1}^M \theta_i = 1 \quad \text{on } \Omega^M, \\ \text{supp } \theta_i \subset \bar{\Omega}_i \quad (1 \leq i \leq M). \end{aligned}$$

REMARK 3.4. The functions θ_i are in general not smooth. In Figure 3.5 a two-dimensional case is illustrated, in which Ω^M consists of three intersecting disks (in this case we have $\mathcal{I}_{\text{int}} = \emptyset$). As a further, more precise, illustration we consider the three-dimensional case of two overlapping balls $\Omega_1 = B((-1, 0, 0); 2)$, $\Omega_2 = B((1, 0, 0); 2)$, with $\Omega^2 := \Omega_1 \cup \Omega_2$. We thus have $\theta_i = \frac{\delta_i}{\delta}$, $i = 1, 2$, $\delta = \delta_1 + \delta_2$.

The intersection of $\partial\Omega^2$ with $\overline{\Omega_1 \cap \Omega_2}$ is the circle $S = \{(0, x_2, x_3) \mid x_2^2 + x_3^2 = 3\}$. The functions θ_i do *not* have a continuous extension to the intersection circle S . Take an accumulation point $x \in S$ and a sequence $(x_n)_{n \in \mathbb{N}} \subset \Omega_1 \setminus \bar{\Omega}_2$ with $\lim_{n \rightarrow \infty} x_n = x$. We then have $\lim_{n \rightarrow \infty} \theta_1(x_n) = 1$. On the other hand, we can take a sequence $(x_n)_{n \in \mathbb{N}} \subset (\Omega_1 \cap \Omega_2)$ with $\lim_{n \rightarrow \infty} x_n = x$ and $\delta_1(x_n) \leq \delta_2(x_n)$, which implies $\limsup_{n \rightarrow \infty} \theta_1(x_n) \leq \frac{1}{2}$. Furthermore, elementary calculation yields that $\theta_i \notin H^1(\Omega_i)$. The key steps for the derivation of this result are outlined in Appendix 8.2.

Related to this we note that the PU introduced above differs from the ones that are typically used in the analysis of domain decomposition methods, cf. [25, Section 3.2]. The reason is that the overlapping covering $(\Omega_i)_{1 \leq i \leq M}$ does not satisfy the key assumption, cf. [25, Assumption 3.1], that for arbitrary i and $x \in \Omega_i$, there exists $\tilde{\delta}_i > 0$ and a j such that $\text{dist}(x, \partial\Omega_j \setminus \partial\Omega^M) \geq \tilde{\delta}_i$ holds.

LEMMA 3.3. *The PU has the following properties:*

$$\|\nabla\theta_i\|_{\infty, \Omega_i} \leq \frac{N_0}{\gamma_{\text{int}}}, \quad \text{for all } i \in \mathcal{I}_{\text{int}}, \quad (3.17)$$

$$\|\nabla\theta_i(x)\| \leq \frac{N_0}{\gamma_{\text{b}} \text{dist}(x, \partial\Omega^M)}, \quad \text{for all } i \in \mathcal{I}_{\text{b}}, x \in \Omega_i. \quad (3.18)$$

Proof. Note that

$$\begin{aligned} \nabla\theta_i(x) &= \frac{\nabla\delta_i(x)}{\delta(x)} - \frac{\delta_i(x)}{\delta(x)} \cdot \frac{\sum_{j=1}^M \nabla\delta_j(x)}{\delta(x)}, \\ &= \frac{\nabla\delta_i(x)}{\delta(x)} \left(1 - \frac{\delta_i(x)}{\delta(x)}\right) - \frac{\delta_i(x)}{\delta(x)} \cdot \frac{\sum_{j \neq i} \nabla\delta_j(x)}{\delta(x)} \quad \text{a.e. on } \Omega^M. \end{aligned}$$

Hence, cf. (3.16) and (3.2),

$$\|\nabla\theta_i(x)\| \leq \frac{1}{\delta(x)} + \frac{\sum_{j \neq i} \|\nabla\delta_j(x)\|}{\delta(x)} \leq \frac{N_0}{\delta(x)}, \quad \text{a.e. on } \Omega^M. \quad (3.19)$$

For $i \in \mathcal{I}_{\text{int}}$ we use (3.5) and obtain the result (3.17). For $i \in \mathcal{I}_{\text{b}}$ we use (3.6), which yields the result (3.18). \square

The results in (3.17), (3.18) show that away from the boundary (i.e., in the subdomain Ω_{int}) the partition of unity functions θ_i are in $W^{1, \infty}$, and towards the boundary the singularity of the gradient of these functions can be controlled by the distance function to the boundary.

4. Analysis of the Schwarz domain decomposition method.

4.1. Pointwise Hardy inequality. In the analysis we need a specific pointwise Hardy inequality, similar to the one derived in e.g. [11, 13]. We introduce some notation. For $f \in L^1(\mathbb{R}^3)$, $B \subset \mathbb{R}^3$ we denote the average by $f_B := \frac{1}{|B|} \int_B f(y) dy$, and the *maximal function* (cf. [23]) by

$$\mathcal{M}(f)(x) := \sup_{r>0} \frac{1}{|B(x; r)|} \int_{B(x; r)} |f(y)| dy.$$

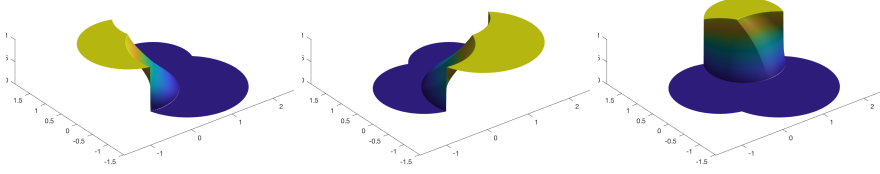


FIG. 3.5. Surface plot of θ_i for a configuration with 3 disks in two dimensions.

A key property is the following ([23], Theorem 1): for all $f \in L^2(\mathbb{R}^3)$:

$$\|\mathcal{M}f\|_{L^2(\mathbb{R}^3)} \leq c_{\mathcal{M}} \|f\|_{L^2(\mathbb{R}^3)}, \quad \text{with } c_{\mathcal{M}} := 10\sqrt{10}. \quad (4.1)$$

In particular, if f is only supported in Ω^M , then the right hand side in (4.1) reduces to $\|f\|_{L^2(\Omega^M)}$.

LEMMA 4.1. Consider a point $x \in \Omega^M$ and a corresponding (arbitrary) exterior point denoted by $b(x) \in \Omega^{M,c}$. Define $d(x) := \|x - b(x)\|$. Let $\gamma(x) > 0$ be such that

$$|B(b(x); d(x)) \cap \Omega^{M,c}| \geq \gamma(x) |B(b(x); d(x))|. \quad (4.2)$$

There exists a constant $c_{\mathcal{H}} > 0$, independent of x and any parameter, such that the following holds for all $u \in C_0^\infty(\Omega^M)$:

$$|u(x)| \leq c_{\mathcal{H}} \frac{d(x)}{\gamma(x)} \mathcal{M}(\|\nabla u\|)(x). \quad (4.3)$$

Proof. Take $u \in C_0^\infty(\Omega^M)$, extended by zero outside Ω^M . Given $x \in \Omega^M$ and a (fixed) $b(x) \in \Omega^{M,c}$, denote $B := B(b(x); d(x))$, and u_B the average of u over B . Further, for this choice of x , take arbitrary $y \in B \cap \Omega^{M,c}$. Using Lemma 7.16 from [10] we obtain

$$\begin{aligned} |u(x)| &= |u(x) - u(y)| \leq |u(x) - u_B| + |u(y) - u_B| \\ &\leq c_1 \left(\int_B \frac{\|\nabla u(z)\|}{\|x - z\|^2} dz + \int_B \frac{\|\nabla u(z)\|}{\|y - z\|^2} dz \right), \end{aligned} \quad (4.4)$$

with $c_1 = \frac{2}{\pi}$. We recall the elementary inequality (e.g., Lemma 3.11.3 in [29]):

$$\frac{1}{|B(x_0; r)|} \int_{B(x_0; r)} \frac{1}{\|y - z\|^2} dy \leq c_2 \frac{1}{\|x_0 - z\|^2} \quad \text{for all } r > 0, x_0, z \in \mathbb{R}^3.$$

(Inspection of the proof of Lemma 3.11.3 in [29] yields $c_2 \leq 14$). Using this, the definition of $\gamma(x)$ and that $B \cap \Omega^{M,c} \subset B \subset B(x; 2d(x))$ we obtain:

$$\begin{aligned} \inf_{y \in B \cap \Omega^{M,c}} \int_B \frac{\|\nabla u(z)\|}{\|y - z\|^2} dz &\leq \frac{1}{|B \cap \Omega^{M,c}|} \int_{B \cap \Omega^{M,c}} \int_B \frac{\|\nabla u(z)\|}{\|y - z\|^2} dz dy \\ &\leq \frac{1}{\gamma(x)} \int_B \frac{1}{|B|} \int_{B \cap \Omega^{M,c}} \frac{1}{\|y - z\|^2} dy \|\nabla u(z)\| dz \\ &\leq \frac{8}{\gamma(x)} \int_B \frac{1}{|B(x; 2d(x))|} \int_{B(x; 2d(x))} \frac{1}{\|y - z\|^2} dy \|\nabla u(z)\| dz \\ &\leq \frac{8c_2}{\gamma(x)} \int_B \frac{\|\nabla u(z)\|}{\|x - z\|^2} dz. \end{aligned}$$

Using this in (4.4) and $\gamma(x) \leq 1$, we get

$$|u(x)| \leq c_1 \left(1 + \frac{8c_2}{\gamma(x)} \right) \int_B \frac{\|\nabla u(z)\|}{\|x-z\|^2} dz \leq \frac{c_1(1+8c_2)}{\gamma(x)} \int_{B(x;2d(x))} \frac{\|\nabla u(z)\|}{\|x-z\|^2} dz.$$

Finally we use the following estimate ([12], Lemma 1):

$$\int_{B(x;r)} \frac{|f(z)|}{\|x-z\|^2} dz \leq c_3 r \mathcal{M}(f)(x) \quad \text{for all } r > 0.$$

(Inspection of the proof in [12] yields $c_3 \leq \frac{4}{\ln 2}$). Combining these results we obtain the estimate (4.3) with $c_{\mathcal{H}} := 2c_1(1+8c_2)c_3$. \square

The result of this lemma is essentially the same as in Proposition 1 in [11] and in Theorem 3.9 in [13]. The only difference is that in the latter results a specific choice for the point $b(x)$ is used, namely a closest point projection of x onto the boundary. Hence, in that case one has $d(x) = \|x - b(x)\| = \text{dist}(x, \partial\Omega^M)$. We will use this specific choice also in the proof of Corollary 4.2 below. In section 4.3, however, we will use a different choice for $b(x)$.

COROLLARY 4.2. *The following holds (recall that $\Omega_b = \cup_{i \in \mathcal{I}_b} \Omega_i$):*

$$\left(\int_{\Omega_b} \left(\frac{u(x)}{\text{dist}(x, \partial\Omega^M)} \right)^2 dx \right)^{\frac{1}{2}} \leq \frac{c_{\mathcal{M}} c_{\mathcal{H}}}{\gamma_f} |u|_{1, \Omega^M} \quad \text{for all } u \in H_0^1(\Omega^M),$$

with $c_{\mathcal{M}}$ as in (4.1), $c_{\mathcal{H}}$ as in (4.3) and γ_f from (3.9).

Proof. Due to density it suffices to consider $u \in C_0^\infty(\Omega^M)$. Take $x \in \Omega_b$ and $i \in \mathcal{I}_b$ such that $x \in \Omega_i$. We take for $b(x) \in \Omega^{M,c}$ the closest point projection on Γ_i as in Indicator 3.5, hence $d(x) = \|x - b(x)\| = \text{dist}(x, \Gamma_i) \leq \text{dist}(x, \partial\Omega^M)$. For $b(x)$ the fatness estimate (3.8) holds. Combining this with the pointwise Hardy estimate (4.3) and (4.1) yields

$$\begin{aligned} \left(\int_{\Omega_b} \left(\frac{u(x)}{\text{dist}(x, \partial\Omega^M)} \right)^2 dx \right)^{\frac{1}{2}} &\leq \left(\int_{\Omega_b} \frac{c_{\mathcal{H}}^2}{\gamma_f^2} \mathcal{M}(\|\nabla u\|)(x)^2 dx \right)^{\frac{1}{2}} \\ &\leq \frac{c_{\mathcal{H}}}{\gamma_f} \|\mathcal{M}(\|\nabla u\|)\|_{L^2(\mathbb{R}^3)} \leq c_{\mathcal{M}} \frac{c_{\mathcal{H}}}{\gamma_f} \|\nabla u\|_{L^2(\mathbb{R}^3)} = \frac{c_{\mathcal{M}} c_{\mathcal{H}}}{\gamma_f} |u|_{1, \Omega^M}, \end{aligned}$$

which completes the proof. \square

4.2. Stability of the subspace decomposition. In the definition of the stability constant s_0 in (2.3) one is free to choose for $v \in H_0^1(\Omega^M)$ any decomposition $v = \sum_{i=1}^M v_i$ with $v_i \in H_0^1(\Omega_i)$. Below we use the natural choice $v_i = \theta_i v$ and analyze this particular decomposition. The result in the following theorem is crucial for the analysis of the Schwarz method.

THEOREM 4.3. *The following estimates hold for all $v \in H_0^1(\Omega^M)$:*

$$\sum_{i=1}^M |\theta_i v|_{1, \Omega_i}^2 \leq C_1 |v|_{1, \Omega^M}^2 + C_2 \sum_{i \in \mathcal{I}_{\text{int}}} \|v\|_{L^2(\Omega_i)}^2 \leq C_1 |v|_{1, \Omega^M}^2 + C_2 N_0 \|v\|_{L^2(\Omega^M)}^2, \quad (4.5)$$

where the constants C_1, C_2 depend only on the local geometry indicators in \mathcal{G}_L^M ; in particular $C_2 = 2N_0^2/\gamma_{\text{int}}^2$.

Proof. The second inequality in (4.5) is an easy consequence of the definition of the overlap indicator N_0 . We derive the first inequality. Take $v \in H_0^1(\Omega^M)$. Using $0 \leq \theta_i \leq 1$ and the definition of N_0 we get

$$\begin{aligned} \sum_{i=1}^M |\theta_i v|_{1, \Omega_i}^2 &= \sum_{i=1}^M \int_{\Omega_i} \|\nabla(\theta_i v)\|^2 dx \leq 2 \sum_{i=1}^M \int_{\Omega_i} \theta_i^2 \|\nabla v\|^2 dx + 2 \sum_{i=1}^M \int_{\Omega_i} \|\nabla \theta_i\|^2 v^2 dx \\ &\leq 2N_0 |v|_{1, \Omega^M}^2 + 2 \sum_{i=1}^M \int_{\Omega_i} \|\nabla \theta_i\|^2 v^2 dx. \end{aligned} \quad (4.6)$$

For estimating the second term in (4.6) we use the partitioning $\{1, \dots, M\} = \mathcal{I}_{\text{int}} \cup \mathcal{I}_{\text{b}}$. Using the result (3.17) we obtain

$$\sum_{i \in \mathcal{I}_{\text{int}}} \int_{\Omega_i} \|\nabla \theta_i\|^2 v^2 dx \leq \left(\frac{N_0}{\gamma_{\text{int}}} \right)^2 \sum_{i \in \mathcal{I}_{\text{int}}} \|v\|_{L^2(\Omega_i)}^2. \quad (4.7)$$

We finally analyze the $\sum_{i \in \mathcal{I}_{\text{b}}}$ part of the sum in (4.6). Take $i \in \mathcal{I}_{\text{b}}$, $x \in \Omega_i$. Using (3.18) and Corollary 4.2 we obtain

$$\begin{aligned} \sum_{i \in \mathcal{I}_{\text{b}}} \int_{\Omega_i} \|\nabla \theta_i\|^2 v^2 dx &\leq \left(\frac{N_0}{\gamma_{\text{b}}} \right)^2 \sum_{i \in \mathcal{I}_{\text{b}}} \int_{\Omega_i} \left(\frac{v}{\text{dist}(x, \partial\Omega^M)} \right)^2 dx \\ &\leq \frac{N_0^3}{\gamma_{\text{b}}^2} \int_{\Omega_{\text{b}}} \left(\frac{v}{\text{dist}(x, \partial\Omega^M)} \right)^2 dx \leq \frac{N_0^3 c_{\mathcal{M}}^2 c_{\mathcal{H}}^2}{\gamma_{\text{b}}^2 \gamma_{\text{f}}^2} |u|_{1, \Omega^M}^2. \end{aligned}$$

Combining this with (4.6), (4.7) completes the proof, yielding

$$\mathbf{C}_1 = 2N_0 \left(1 + \frac{N_0^2 c_{\mathcal{M}}^2 c_{\mathcal{H}}^2}{\gamma_{\text{b}}^2 \gamma_{\text{f}}^2} \right).$$

□

The result (4.5) implies that, although θ_i , $i \in \mathcal{I}_{\text{b}}$, is *not* necessarily in $H^1(\Omega_i)$ (Remark 3.4), for $v \in H_0^1(\Omega^M)$ the product $\theta_i v$ is an element of $H^1(\Omega_i)$. In this product the singularity of $\nabla \theta_i$ at the boundary can be controlled due to the property $v|_{\partial\Omega^M} = 0$.

COROLLARY 4.4. *Assume $\mathcal{I}_{\text{int}} = \emptyset$. The estimate*

$$\sum_{i=1}^M |\theta_i v|_{1, \Omega_i}^2 \leq \mathbf{C}_1 |v|_{1, \Omega^M}^2, \quad \text{for all } v \in H_0^1(\Omega^M), \quad (4.8)$$

holds, where the constant \mathbf{C}_1 depends only on the local geometry indicators in \mathcal{G}_L^M .

COROLLARY 4.5. *For all $v \in H_0^1(\Omega^M)$ we have*

$$\theta_i v \in H_0^1(\Omega_i), \quad i = 1, \dots, M. \quad (4.9)$$

Furthermore,

$$\sum_{i=1}^M H_0^1(\Omega_i) = H_0^1(\Omega^M) \quad (4.10)$$

holds.

Proof. Take $v \in H_0^1(\Omega^M)$ and $i \in \mathcal{I}$. From Theorem 4.3 it follows that $\theta_i v \in H^1(\Omega_i)$. Define $\Gamma_i := \partial\Omega_i \cap \partial\Omega^M$, i.e., $\partial\Omega_i = \Gamma_i \cup (\partial\Omega_i \setminus \Gamma_i)$. If $\text{meas}_2(\Gamma_i) > 0$, then on Γ_i we have (due to the trace theorem) $(\theta_i v)|_{\Gamma_i} = (\theta_i)|_{\Gamma_i} v|_{\Gamma_i} = 0$, due to $v|_{\partial\Omega^M} = 0$ and boundedness of θ_i . For $x \in \partial\Omega_i \setminus \Gamma_i$ we have $\theta_i(x) = 0$, hence, $(\theta_i v)|_{(\partial\Omega_i \setminus \Gamma_i)} = 0$. This completes the proof of (4.9).

Take $v \in H_0^1(\Omega^M)$ and note that $v = \left(\sum_{i=1}^M \theta_i\right)v = \sum_{i=1}^M (\theta_i v)$, with $\theta_i v \in H_0^1(\Omega_i)$. This proves the result (4.10). \square

The result (4.10) implies that the assumption used in Lemma 2.1 is satisfied:

COROLLARY 4.6. $\sum_{i=1}^M H_0^1(\Omega_i)$ is closed in $H_0^1(\Omega^M)$.

The remaining task is to bound the term $\sum_{i \in \mathcal{I}_{int}} \|v\|_{L^2(\Omega_i)}^2$ in (4.5). In section 4.3 we derive a Poincaré estimate in which this term is bounded in terms of the desired norm $|v|_{1, \Omega^M}$. This immediately implies a bound for the stability constant s_0 .

4.3. Poincaré estimate and main result. In this section we derive a main result, namely an estimate for the stability quantity s_0 in Theorem 4.8 below. We summarize the different parameters that have been introduced above and play a role in this main result. These are:

local geometry indicators, cf. Section 3: $\mathcal{G}_L^M := \{N_{\max}, N_0, \gamma_{\text{int}}^{-1}, \gamma_{\text{b}}^{-1}, \gamma_{\text{f}}^{-1}\}$,

global exterior fatness indicator, cf. (3.14): d_F ,

generic Hardy constants, cf. (4.1), (4.3): $c_{\mathcal{M}}, c_{\mathcal{H}}$.

We use the pointwise Hardy inequality in Lemma 4.1 in combination with the *global* exterior fatness property as in indicator 3.6 to derive a bound for the term $\|v\|_{L^2(\Omega^M)}$ in terms of $|v|_{1, \Omega^M}$. Note that the optimal constant that occurs in such an estimate is the inverse of the smallest eigenvalue of the Laplace eigenvalue problem in $H_0^1(\Omega^M)$. In the following, we will find a geometry-dependent upper bound of this constant, or equivalently, a lower bound of the smallest eigenvalue, that depends on geometric features of the domain Ω^M . For this we use the global fatness indicator in (3.14) which characterizes certain global geometry properties of Ω^M (which then, for example, distinguishes a linear chain from a globular topology).

LEMMA 4.7. *The following estimate holds for all $u \in H_0^1(\Omega^M)$:*

$$\|u\|_{L^2(\Omega^M)} \leq c_{\mathcal{H}} c_{\mathcal{M}} d_F |u|_{1, \Omega^M},$$

with the global fatness indicator d_F as in (3.14).

Proof. Due to density it suffices to consider $u \in C_0^\infty(\Omega^M)$. For $x \in \Omega^M$ we take the exterior point $b(x)$ and γ_F as in Indicator 3.6. Using Lemma 4.1 and (4.1) we obtain with $d(x) := \|b(x) - x\|$:

$$\begin{aligned} \|u\|_{L^2(\Omega^M)} &= \left(\int_{\Omega^M} u(x)^2 dx \right)^{\frac{1}{2}} \leq \frac{c_{\mathcal{H}}}{\gamma_F} \max_{x \in \Omega^M} d(x) \left(\int_{\Omega^M} \mathcal{M}(\|\nabla u\|)(x)^2 dx \right)^{\frac{1}{2}} \\ &\leq c_{\mathcal{H}} d_F \|\mathcal{M}(\|\nabla u\|)\|_{L^2(\mathbb{R}^3)} \leq c_{\mathcal{H}} c_{\mathcal{M}} d_F \|\nabla u\|_{L^2(\mathbb{R}^3)} = c_{\mathcal{H}} c_{\mathcal{M}} d_F |u|_{1, \Omega^M}, \end{aligned}$$

which proves the result. \square

REMARK 4.1. It follows therefore that

$$c_{\mathcal{H}}^{-1} c_{\mathcal{M}}^{-1} d_F^{-1}$$

is a lower bound of the lowest eigenvalue of the Laplace eigenvalue problem in $H_0^1(\Omega^M)$, where d_F accounts for the geometry of the domain.

We derive a bound for the stability quantity s_0 , cf. (2.1):

THEOREM 4.8. *For the stability quantity s_0 the following bounds hold, with C_3, C_4 , constants that depend only on the local geometry indicators in \mathcal{G}_L^M and on $c_{\mathcal{H}}, c_{\mathcal{M}}$. If $\mathcal{I}_{\text{int}} = \emptyset$ holds we have*

$$s_0 \leq C_3. \quad (4.11)$$

If $\mathcal{I}_{\text{int}} \neq \emptyset$ we have

$$s_0 \leq C_3 + C_4 d_F^2. \quad (4.12)$$

Proof. For $v \in H_0^1(\Omega^M)$ we define $\hat{v}_j := \theta_j v \in H_0^1(\Omega_j)$, i.e., $v = \sum_{j=1}^M \hat{v}_j$. Note that:

$$\begin{aligned} \inf_{\sum_{j=1}^M v_j = v} \sum_{i=1}^M \left| P_i \sum_{j=i+1}^M v_j \right|_{1, \Omega_i}^2 &\leq \sum_{i=1}^M \left| P_i \sum_{j=i+1}^M \hat{v}_j \right|_{1, \Omega_i}^2 = \sum_{i=1}^M \left| P_i \sum_{j \in \mathcal{N}_i} \hat{v}_j \right|_{1, \Omega_i}^2 \\ &\leq \sum_{i=1}^M \left| \sum_{j \in \mathcal{N}_i} \hat{v}_j \right|_{1, \Omega^M}^2 \leq N_{\max} \sum_{i=1}^M \sum_{j \in \mathcal{N}_i} |\hat{v}_j|_{1, \Omega_j}^2 \\ &\leq N_{\max}^2 \sum_{i=1}^M |\hat{v}_i|_{1, \Omega_i}^2. \end{aligned}$$

For estimating the term $\sum_{i=1}^M |\hat{v}_i|_{1, \Omega_i}^2$ we apply Theorem 4.3. If $\mathcal{I}_{\text{int}} = \emptyset$ we use Corollary 4.4 and then, using the definition of s_0 , obtain the result in (4.11), with $C_3 := N_{\max}^2 C_1$ and C_1 as in Theorem 4.3. If $\mathcal{I}_{\text{int}} \neq \emptyset$ we apply Theorem 4.3 and Lemma 4.7 and obtain the result (4.12), with $C_4 = N_{\max}^2 C_2 N_0 c_{\mathcal{H}}^2 c_{\mathcal{M}}^2$ (C_2 as in Theorem 4.3). \square

Note that the constants C_3, C_4 depend only on the local geometry indicators in \mathcal{G}_L^M (and the generic constants $c_{\mathcal{H}}, c_{\mathcal{M}}$). The information on the global geometry of Ω^M enters (only) through the global fatness indicator d_F . This proves that in cases where one has a very large number of balls ($M \rightarrow \infty$) but moderate values of the geometry indicators in \mathcal{G}_L^M and of d_F , the convergence of the Schwarz domain decomposition method is expected to be fast. Furthermore, if the number M of balls is increased, but the values of these local geometry indicators and of d_F are uniformly bounded with respect to M , the convergence of the Schwarz domain decomposition method does not deteriorate. A worst case scenario (globular domain) is $d_F \sim M^{\frac{1}{3}}$ ($M \rightarrow \infty$). In that case, due to $|E|_{1, \Omega^M} = (1 - \frac{1}{1+s_0})^{\frac{1}{2}}$, the number of iterations ℓ of the Schwarz domain decomposition method that is needed to obtain a given accuracy, scales like

$$\ell \sim s_0 \sim d_F^2 \sim M^{\frac{2}{3}}.$$

A symmetrized version of the Schwarz domain decomposition method can be combined with a conjugate gradient acceleration, cf. [26]. This results in an improved scaling of the number of iterations, namely $\ell \sim M^{\frac{1}{3}}$.

5. An additional coarse global space. In case of a globular domain Ω^M both numerical experiments and the theory presented above show that the convergence of the Schwarz domain decomposition method can be slow for very large M . As is well-known from the field of domain decomposition methods (and subspace correction methods) this deterioration can be avoided by introducing a suitable “coarse level space”. In this section we propose such a space:

$$V_0 := \text{span}\{\theta_i \mid i \in \mathcal{I}_{\text{int}}\} \subset H_0^1(\Omega^M)$$

(we assume $\mathcal{I}_{\text{int}} \neq \emptyset$, otherwise we use Theorem 4.8, Eqn. (4.11)). The corresponding projection $P_0 : H_0^1(\Omega) \rightarrow V_0$ is such that $a(P_0 v, w_0) = a(v, w_0)$ for all $w_0 \in V_0$. In the definition of V_0 it is important to restrict to $i \in \mathcal{I}_{\text{int}}$ (instead of $i \in \mathcal{I}$) because for $i \in \mathcal{I}_{\text{b}}$ the partition of unity functions θ_i are not necessarily contained in $H_0^1(\Omega^M)$. In the Schwarz method one then has to solve for an additional correction in V_0 : $e_0 \in V_0$ such that

$$a(e_0, v_0) = f(v_0) - a(u_{i-1}^{\ell-1}, v_0) \quad \text{for all } v_0 \in V_0.$$

Using the basis $(\theta_i)_{i \in \mathcal{I}_{\text{int}}}$ in V_0 this results in a sparse linear system of (maximal) dimension $\sim M \times M$. In practice this coarse global system will be solved approximately by a multilevel technique, cf. Remark 5.1 below.

The analysis of the method with the additional correction in the space V_0 is again based on Lemma 2.1, which is also valid if we use the decomposition $H_0^1(\Omega) = V_0 + \sum_{i=1}^M H_0^1(\Omega_i)$ (and include $i = 0$ in the sum in Lemma 2.1). For the analysis (only) we need a “suitable” linear mapping $Q_0 : H_0^1(\Omega^M) \rightarrow V_0$. A natural choice is the following:

$$Q_0 v = \sum_{i \in \mathcal{I}_{\text{int}}} \bar{v}_i \theta_i, \quad \bar{v}_i := \frac{1}{|\Omega_i|} \int_{\Omega_i} v \, dx.$$

For deriving properties of this mapping we introduce additional notation:

$$\begin{aligned} \mathcal{N}_i^* &:= \{j \in \mathcal{I}_{\text{int}} \mid \Omega_j \cap \Omega_i \neq \emptyset\} \subset \mathcal{N}_i, \quad i \in \mathcal{I}, \\ \mathcal{I}_{\text{int}}^* &:= \{i \in \mathcal{I}_{\text{int}} \mid [\Omega_j \cap \Omega_i \neq \emptyset] \Rightarrow j \in \mathcal{I}_{\text{int}}\}, \quad \mathcal{I}_{\text{b}}^* = \mathcal{I} \setminus \mathcal{I}_{\text{int}}^*, \\ \Omega_i^* &:= \cup_{j \in \mathcal{N}_i^* \cup \{i\}} \Omega_j, \quad i \in \mathcal{I}. \end{aligned}$$

The index set $\mathcal{I}_{\text{int}}^*$ contains those $i \in \mathcal{I}_{\text{int}}$ for which the ball Ω_i has only neighboring balls that are interior balls. For $i \in \mathcal{I}_{\text{int}}^*$ we have $\mathcal{N}_i^* = \mathcal{N}_i$. We also need two further local geometry indicators:

$$N_0^* \text{ is the smallest integer such that: } \max_{x \in \Omega^M} \text{card}\{j \mid x \in \Omega_j^*\} \leq N_0^*. \quad (5.1)$$

$$q_i := \max_{j \in \mathcal{N}_i^*} \frac{|\Omega_i|}{|\Omega_j|}, \quad q_{\max} := \max_{i \in \mathcal{I}} q_i. \quad (5.2)$$

The indicator in (5.1) is a variant of the maximal overlap indicator N_0 in (3.2) (with Ω_j replaced by Ω_j^*) and q_{\max} essentially measures the maximal variation in radii of neighboring balls. Below we use the standard Sobolev norm on $H^1(\Omega_i)$, denoted by $\|\cdot\|_{1, \Omega_i}$.

LEMMA 5.1. *There are constants $\mathbf{B}_1, \mathbf{B}_2$, depending only on the local geometry indicators $N_0, N_0^*, \gamma_{\text{int}}, q_{\max}, R_{\max}, N_{\max}$ such that:*

$$\|v - Q_0 v\|_{1, \Omega_i} \leq |v|_{1, \Omega_i} + \mathbf{B}_1 \|v\|_{L^2(\Omega_i^*)} \quad \text{for all } i \in \mathcal{I}, \quad v \in H^1(\Omega_i^*), \quad (5.3)$$

$$\|v - Q_0 v\|_{1, \Omega_i} \leq \mathbf{B}_2 |v|_{1, \Omega_i^*} \quad \text{for all } i \in \mathcal{I}_{\text{int}}^*, \quad v \in H^1(\Omega_i^*). \quad (5.4)$$

Proof. Take $i \in \mathcal{I}$, $v \in H^1(\Omega_i^*)$. Note $(Q_0 v)|_{\Omega_i} = (\sum_{j \in \mathcal{N}_i^*} \bar{v}_j \theta_j)|_{\Omega_i}$. Since $\mathcal{N}_i^* \subset \mathcal{I}_{\text{int}}$ we have $\|\nabla \theta_j\|_{\infty, \Omega_i} \leq \frac{N_0}{\gamma_{\text{int}}}$ for $j \in \mathcal{N}_i^*$, hence, $\|\theta_j\|_{1, \Omega_i}^2 \leq |\Omega_i| \left(1 + \left(\frac{N_0}{\gamma_{\text{int}}}\right)^2\right)$. Furthermore, $|\bar{v}_j| \leq |\Omega_j|^{-\frac{1}{2}} \|v\|_{L^2(\Omega_j)}$. Using this we obtain

$$\begin{aligned} \|v - Q_0 v\|_{1, \Omega_i} &\leq \|v\|_{1, \Omega_i} + \left\| \sum_{j \in \mathcal{N}_i^*} \bar{v}_j \theta_j \right\|_{1, \Omega_i} \leq |v|_{1, \Omega_i} + \|v\|_{L^2(\Omega_i)} + \sum_{j \in \mathcal{N}_i^*} |\bar{v}_j| \|\theta_j\|_{1, \Omega_i} \\ &\leq |v|_{1, \Omega_i} + \|v\|_{L^2(\Omega_i)} + \left(1 + \frac{N_0}{\gamma_{\text{int}}}\right) \max_{j \in \mathcal{N}_i^*} \left(\frac{|\Omega_i|}{|\Omega_j|}\right)^{\frac{1}{2}} \sum_{j \in \mathcal{N}_i^*} \|v\|_{L^2(\Omega_j)} \\ &\leq |v|_{1, \Omega_i} + \mathbf{B}_1 \|v\|_{L^2(\Omega_i^*)}, \end{aligned}$$

with $\mathbf{B}_1 = 1 + \left(1 + \frac{N_0}{\gamma_{\text{int}}}\right) q_{\max}^{\frac{1}{2}} N_0^*$, which proves the result (5.3).

Now take $i \in \mathcal{I}_{\text{int}}^*$, hence $(\sum_{j \in \mathcal{N}_i^*} \theta_j)|_{\Omega_i} = 1$. This implies that for an arbitrary constant \hat{c} we have

$$(Q_0 \hat{c})|_{\Omega_i} = \left(\sum_{j \in \mathcal{N}_i^*} \hat{c} \theta_j\right)|_{\Omega_i} = \hat{c}.$$

Using the estimate from above yields, for arbitrary $v \in H^1(\Omega_i^*)$

$$\|v - Q_0 v\|_{1, \Omega_i} = \|v - \hat{c} - Q_0(v - \hat{c})\|_{1, \Omega_i} \leq |v|_{1, \Omega_i} + \mathbf{B}_1 \|v - \hat{c}\|_{L^2(\Omega_i^*)}$$

for an arbitrary constant \hat{c} . Take $\hat{c} := \frac{1}{|\Omega_i^*|} \int_{\Omega_i^*} v \, dx$, hence $\int_{\Omega_i^*} v - \hat{c} \, dx = 0$. We now apply a Friedrichs inequality to the term $\|v - \hat{c}\|_{L^2(\Omega_i^*)}$. The domain Ω_i^* has a simple structure, namely the union of a few (at most N_{\max}) balls. Hence the constant in the Friedrichs inequality can be quantified. Theorem 3.2 in [28] yields an estimate in which the constant c_F depends only on the number N_{\max} and the diameters R_j , $j \in \mathcal{N}_i^*$. This yields

$$\|v - \hat{c}\|_{L^2(\Omega_i^*)} \leq c_F(N_{\max}, R_{\max}) |v|_{1, \Omega_i^*}.$$

Hence, (5.4) holds, with $\mathbf{B}_2 = 1 + \mathbf{B}_1 c_F(N_{\max}, R_{\max})$. \square

In the derivation of the main result in Theorem 5.3 below we have to control $\|v\|_{L^2(\Omega_b^*)}$, on a ‘‘boundary strip’’ $\Omega_b^* := \cup_{i \in \mathcal{I}_b^*} \Omega_i^*$, in terms of $|v|_{1, \Omega^M}$. For this we use arguments, based on the Hardy inequality, very similar to the ones used in the previous sections. Denote the union of all balls that have a nonzero overlap with Ω_i by $\Omega_i^e := \cup_{j \in \mathcal{N}_i} \Omega_j$. Note that for $i \in \mathcal{I}_b^*$ the ball Ω_i has an overlapping neighboring ball $\Omega_j \subset \Omega_b$, and thus $\partial\Omega_i^e \cap \partial\Omega^M =: \Gamma_i^e \neq \emptyset$. We need a variant of the local exterior fatness Indicator 3.5. For $i \in \mathcal{I}_b^*$ and $x \in \Omega_i^*$ let $p(x)$ be the closest point projection on Γ_i^e . Let $\hat{c}_i^* > 0$ be such that

$$|B(p(x); \|p(x) - x\|) \cap \Omega^{M,c}| \geq \hat{c}_i^* |B(p(x), \|p(x) - x\|)|, \quad \text{for all } x \in \Omega_i^*, \quad (5.5)$$

cf. (3.8), and define

$$\gamma_f^* := \min_{i \in \mathcal{I}_b^*} \hat{c}_i^* > 0. \quad (5.6)$$

The quantity γ_f^* is a *local* indicator because \hat{c}_i^* depends only on a small neighbourhood of Ω_i^e .

LEMMA 5.2. *There exists a constant B_3 , depending only on the local geometry parameters γ_f^* and R_{\max} , such that*

$$\|v\|_{L^2(\Omega_b^*)} \leq B_3 |v|_{1, \Omega^M} \quad \text{for all } v \in H_0^1(\Omega^M). \quad (5.7)$$

Proof. For $x \in \Omega_b^*$ we have $d(x) = \|x - p(x)\| \leq 4R_{\max}$. Using (5.5) and the Hardy inequality in Lemma 4.1 we obtain, for $v \in C_0^\infty(\Omega^M)$:

$$|v(x)| \leq \hat{c} \mathcal{M}(\|\nabla v\|)(x), \quad \hat{c} := c_{\mathcal{H}} \frac{4R_{\max}}{\gamma_f^*}.$$

Combining this with (4.1) yields

$$\|v\|_{L^2(\Omega_b^*)} \leq \hat{c} c_{\mathcal{M}} |v|_{1, \Omega^M}.$$

Application of a density argument completes the proof. \square

Using the two lemmas above we derive the following main result for the stability quantity s_0 .

THEOREM 5.3. *For the stability constant s_0 the bound*

$$s_0 \leq C_0$$

holds, with a constant C_0 that depends only on the local geometry indicators in \mathcal{G}_L^M and on N_0^ , q_{\max} , γ_f^* .*

Proof. For $v \in H_0^1(\Omega^M)$ we define $\hat{v}_0 = Q_0 v$, $\hat{v}_i := \theta_i(v - Q_0 v) \in H_0^1(\Omega_i)$, i.e., $v = \sum_{i=0}^M \hat{v}_i$, and $\sum_{i=1}^M \hat{v}_i = v - \hat{v}_0$. Using Theorem 4.3 we obtain, along the same lines as in the proof of Theorem 4.8, with $\Omega_0 := \Omega^M$,

$$\begin{aligned} s_0 &= \inf_{\sum_{j=0}^M v_j = v} \sum_{i=0}^M \left| P_i \sum_{j=i+1}^M v_j \right|_{1, \Omega_i}^2 \leq \sum_{i=0}^M \left| P_i \sum_{j=i+1}^M \hat{v}_j \right|_{1, \Omega_i}^2 \\ &\leq |P_0(v - \hat{v}_0)|_{1, \Omega^M}^2 + \sum_{i=1}^M \left| P_i \sum_{j \in \mathcal{N}_i} \hat{v}_j \right|_{1, \Omega_i}^2 \leq |v - \hat{v}_0|_{1, \Omega^M}^2 + \sum_{i=1}^M \left| \sum_{j \in \mathcal{N}_i} \hat{v}_j \right|_{1, \Omega_i}^2 \\ &\leq |v - \hat{v}_0|_{1, \Omega^M}^2 + N_{\max}^2 \sum_{i=1}^M |\hat{v}_i|_{1, \Omega_i}^2 \\ &\leq (1 + N_{\max}^2 C_1) |v - Q_0 v|_{1, \Omega^M}^2 + N_{\max}^2 C_2 \sum_{i \in \mathcal{I}_{\text{int}}} \|v - Q_0 v\|_{L^2(\Omega_i)}^2. \end{aligned}$$

Using

$$|v - Q_0 v|_{1, \Omega^M}^2 \leq \sum_{i \in \mathcal{I}_{\text{int}}^*} |v - Q_0 v|_{1, \Omega_i}^2 + \sum_{i \in \mathcal{I}_b^*} |v - Q_0 v|_{1, \Omega_i}^2,$$

and

$$\sum_{i \in \mathcal{I}_{\text{int}}} \|v - Q_0 v\|_{L^2(\Omega_i)}^2 \leq \sum_{i \in \mathcal{I}_{\text{int}}^*} \|v - Q_0 v\|_{L^2(\Omega_i)}^2 + \sum_{i \in \mathcal{I}_b^*} \|v - Q_0 v\|_{L^2(\Omega_i)}^2,$$

we obtain, with $\tilde{c} := \max\{1 + N_{\max}^2 C_1, N_{\max}^2 C_2\}$:

$$s_0 \leq \tilde{c} \left(\sum_{i \in \mathcal{I}_{\text{int}}^*} \|v - Q_0 v\|_{1, \Omega_i}^2 + \sum_{i \in \mathcal{I}_b^*} \|v - Q_0 v\|_{1, \Omega_i}^2 \right). \quad (5.8)$$

For the term $\sum_{i \in \mathcal{I}_{\text{int}}^*}$ we use the result (5.4):

$$\sum_{i \in \mathcal{I}_{\text{int}}^*} \|v - Q_0 v\|_{1, \Omega_i}^2 \leq \mathbf{B}_2^2 \sum_{i \in \mathcal{I}_{\text{int}}^*} |v|_{1, \Omega_i^*}^2 \leq \mathbf{B}_2^2 N_0^* |v|_{1, \Omega^M}^2.$$

For the term $\sum_{i \in \mathcal{I}_b^*}$ we use the result (5.3):

$$\begin{aligned} \sum_{i \in \mathcal{I}_b^*} \|v - Q_0 v\|_{1, \Omega_i}^2 &\leq 2 \sum_{i \in \mathcal{I}_b^*} |v|_{1, \Omega_i}^2 + 2\mathbf{B}_1^2 \sum_{i \in \mathcal{I}_b^*} \|v\|_{L^2(\Omega_i^*)}^2 \\ &\leq 2N_0 |v|_{1, \Omega^M}^2 + 2\mathbf{B}_1^2 N_0^* \|v\|_{L^2(\Omega_b^*)}^2. \end{aligned}$$

Finally, the term $\|v\|_{L^2(\Omega_b^*)}$ can be estimated as in Lemma 5.2. Combining these results completes the proof. \square

REMARK 5.1. The Schwarz domain decomposition method analyzed in this paper is not feasible in practice, because it iterates “on the continuous level”. In every iteration of the method one has to solve *exactly* a Poisson equation (with homogeneous Dirichlet data) on each of the balls Ω_i , $i = 1, \dots, M$. If the coarse global space V_0 is used, this requires the exact solution of a sparse linear system with a matrix of dimension approximately $M \times M$. Note that the local problems are PDEs, whereas the global one is a sparse linear system. In practice, the exact solves on the balls are replaced by inexact ones, which can be realized very efficiently using harmonic polynomials in terms of spherical coordinates using spherical harmonics. These inexact local solves define a *discretization* of the original global PDE. If the coarse global space is used, the resulting linear system can be solved using a multilevel technique, which then requires computational work for the coarse space correction that is linear in M . Numerical experiments (so far only for the case without coarse global space) indicate that the method with inexact local solves has convergence properties very similar to the one with exact solves that is analyzed in this paper as the local discretization can be systematically improved. An analysis of the method with inexact local and global solves is a topic for future research. We expect that such an analysis can be done using tools and results from the literature on subspace correction methods, because in that framework the effect of inexact solves on the rate of convergence of the resulting solver has been thoroughly studied, cf. e.g. [26].

REMARK 5.2. In a setting with very large scale problems solved on parallel architectures, the *additive* Schwarz domain decomposition method, also called “parallel subspace correction method” [26], is (much) more efficient than the Schwarz domain decomposition method considered in this paper (“successive subspace correction method”). We indicate how the results obtained in this paper can be applied to the setting of an additive Schwarz method. We first consider the case without a coarse global space. In the additive method one obtains a *preconditioned system* with a symmetric positive definite operator $T := \sum_{j=1}^M P_j$, cf. [27, 25]. The quality of the additive Schwarz preconditioner is measured using the condition number $\text{cond}(T) = \frac{\lambda_{\max}(T)}{\lambda_{\min}(T)}$. A (sharp) bound for this condition number is derived in [25, Theorem 2.7]. This bound depends on three parameters, denoted by ω , $\rho(\mathcal{E})$, C_0 , cf. [25] for definitions. In the case of “exact subspace solvers” that we consider, we have $\omega = 1$. We use a (stable) decomposition as in Theorem 4.3. Due to $a(\theta_i v, \theta_j v) = 0$ for all $j \notin \mathcal{N}_i$ it follows that $\rho(\mathcal{E}) \leq N_{\max}$. The parameter C_0 quantifies the stability of the decomposition. For this essentially the same bounds as for s_0 in Theorems 4.8 and 5.3 hold.

6. Numerical experiments. We only present a few numerical examples in order to complement results already available in the literature. In [1] results of numerical experiments are presented which show that the method scales linearly in the number of balls in linear chains of same-sized balls in three dimensions. In [4] results that show linear scaling are given for more general essentially one-dimensional structures, but limited to two spatial dimensions. Numerical results of the domain decomposition method applied to real molecules are presented in [19], more precisely treating alanine chains and compounds of one to several hemoglobin units. Further [6] sheds light on the difference in terms of the number of iterations between chain-like versus globular biologically relevant molecules and the sensitivity with respect to the radii R_i .

Here we restrict to a few theoretical scenarios, i.e. we consider the center of the balls to lie on a regular unit lattice $\mathcal{L}_{\mathbf{n}}$, for $\mathbf{n} = (n_x, n_y, n_z)$, defined by $\mathcal{L}_{\mathbf{n}} = [1, n_x] \times [1, n_y] \times [1, n_z] \cap \mathbb{N}^3$. We take all radii the same and equal to 0.9 in order that no inner holes appear in the structures and that there is significant overlap between neighbouring balls. We consider three different cases:

- Case 1: n_x, n_y are fix and $n_z = n \in \mathbb{N}$ is growing. This represents a lattice that is growing in one direction.
- Case 2: n_x is fix and $n_y = n_z = n \in \mathbb{N}$ is growing. This represents a lattice that is growing in two directions.
- Case 3: $n_x = n_y = n_z = n \in \mathbb{N}$ is growing. This represents a lattice that is growing in all three directions.

Case 3 differs from the first two cases in the sense that for the global fatness indicator d_F we have, in the limit $n \rightarrow \infty$, $d_F \sim n$ in former case, whereas for Case 1 and 2, d_F is uniformly bounded (with respect to n), but depends on n_x, n_y and n_x , respectively.

Since the contraction behaviour only depends on the operator, we consider the simple setting of $f = 0$, i.e. $-\Delta u = 0$ with trivial solution, and observe the contraction of a given non-trivial starting function u^0 to $u \equiv 0$. Indeed, u^0 is chosen equal to one in the inner balls of the domain and smoothly decreases to zero boundary values within the boundary layer of balls. The local problems are solved using spherical harmonics times a radial monomial. Indeed, since we know a priori that the solution is harmonic we use a spectral method with harmonic basis functions of the form $r^k Y_{km}(\theta, \varphi)$, where (r, θ, φ) denote the spherical coordinates with respect to the balls center and Y_{km} the real-valued spherical harmonics. We choose the degree of spherical harmonics high enough such that the approximation error is not affecting the iterative process.

Figure 6.1 illustrates the number of iterations of the algorithm presented in (2.2) with and without coarse correction to reach a relative error criterion $|u^\ell|_{1, \Omega^M} < 10^{-6} |u^0|_{1, \Omega^M}$. As predicted by the theory presented in this paper, we have a bounded number of iterations in Case 1 and 2 (with dependency on n_x (and n_y in Case 2)), while Case 3 shows a growing number of iterations that is approximately linear in n if no coarse global space correction is employed. On the other hand, all cases show a bounded number of iterations, as predicted by the theory, if the coarse global space correction is employed.

7. Conclusion and outlook. In this paper we presented an analysis of the rate of convergence of the overlapping Schwarz domain decomposition method applied to the Poisson problem on a special family of domains, motivated by applications in implicit solvation models in computational chemistry. The analysis uses the framework of subspace correction methods, in which the contraction number of the error propagation operator (in the natural energy norm) can be expressed in only one stability parameter, namely s_0 appearing in Lemma 2.1. We investigate how this stability pa-

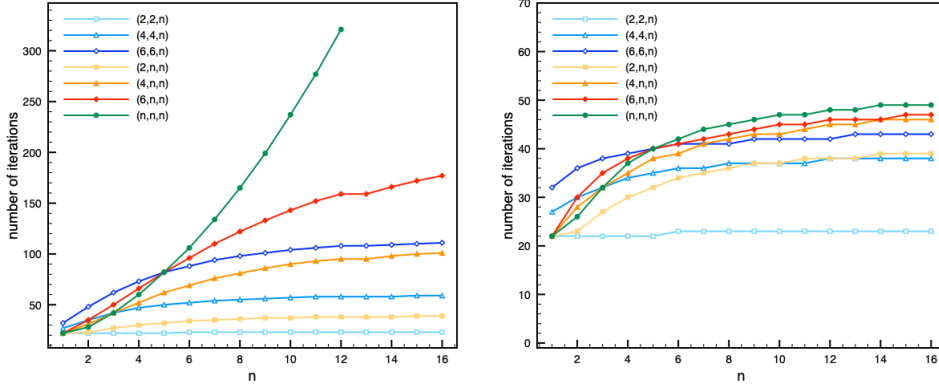


FIG. 6.1. Number of iterations of the Algorithm (2.2) to reach a fixed error tolerance for different lattice-structures labelled by the description (n_x, n_y, n_z) without (left) and with (right) coarse correction.

parameter depends on relevant geometric properties of the domains, such as the amount of overlap between neighbouring balls and the exterior fatness of the domain. The latter plays a key role in the analysis of a Poincaré inequality. To formalize the dependence of the constants in the estimates on relevant geometric properties we introduced local geometry indicators, cf. (3.10), and a global geometry indicator d_F (3.14). In view of our applications it is reasonable to assume that the local indicators are uniformly (in the number of subdomains) bounded. We derive bounds for the stability parameter s_0 as presented in the main Theorem 4.8. The results of this theorem show that the rate of convergence of the overlapping Schwarz domain decomposition method can deteriorate in situations with very large d_F values and remains constant for (possibly complex and non-trivial) geometrical structures where d_F remains constant, which is the case in the majority of cases when dealing with biochemical molecules. This result provides therefore a theoretical justification of the performance of the solvers observed in implicit solvation models. In cases where d_F is large, the efficiency of the method can be significantly improved by using an additional coarse global space, as explained in section 5. Including such a space results in a uniform bound for s_0 that in particular does not depend on d_F , cf. Theorem 5.3.

In this paper we restricted the analysis to the case with exact subspace solvers, both for the local Poisson problems in $H_0^1(\Omega_i)$ and the Poisson problem in the coarse global space V_0 . In future work we want to study the effect of inexact solvers by means of a local discretization error. In recent years the method without the coarse global space has been used for the efficient simulation of many complex applications in the field of implicit solvation models. So far we did not perform a systematic numerical study of the method with the coarse global space. We plan to do this in the near future.

8. Appendix. In this appendix we give a proof of Lemma 3.2 and a derivation of the result stated in Remark 3.4.

8.1. Proof of Lemma 3.2. *Proof.* Define $\alpha = \frac{\pi}{2} - \beta^\infty$, where β^∞ is the minimal angle (half of the aperture) constant of Assumption **(A4)**, and

$$\varepsilon := R_{\min}^\infty (1 - \sin(\alpha)).$$

We introduce the splitting of Ω_b into

$$\Omega_\varepsilon = \{x \in \Omega_b \mid \delta(x) < \varepsilon\}, \quad \Omega_\varepsilon^c = \{x \in \Omega_b \mid \delta(x) \geq \varepsilon\}.$$

First, for $x \in \Omega_\varepsilon^c$ we have $\frac{\delta(x)}{\text{dist}(x, \partial\Omega^M)} \geq \frac{\varepsilon}{2R_{\max}^\infty}$. Hence,

$$\delta(x) \geq \frac{R_{\min}^\infty(1-\sin(\alpha))}{2R_{\max}^\infty} \text{dist}(x, \partial\Omega^M) \quad \text{for all } x \in \Omega_\varepsilon^c. \quad (8.1)$$

Second, we consider $x \in \Omega_\varepsilon$. We start with some preliminary consideration. We denote by $\sphericalangle(v, w) := \arccos\left(\frac{v \cdot w}{\|v\| \|w\|}\right)$ the angle between two vectors $v, w \in \mathbb{R}^3$. The circular cone with apex $y \in \mathbb{R}^3$, axis $w \in \mathbb{R}^3$ and aperture 2α is denoted by

$$K_y(w, \alpha) = \left\{ z = y + v \in \mathbb{R}^3 \mid v \in \mathbb{R}^3, \sphericalangle(w, v) \leq \alpha \right\}.$$

Let $y = p(x) \in \partial\Omega^M$ denote one of the closest points of x on $\partial\Omega^M$. Following the notation introduced in [9], let $\mathbf{i} = \mathcal{I}(y) = \{i_1, \dots, i_r\}$ be the maximal set of indices such that $y \in \bigcap_{i \in \mathcal{I}(y)} \partial\Omega_i$.

If $\mathbf{i} = \mathcal{I}(y) = \{i_1\}$, i.e., if y is contained on a spherical patch and only belonging to one sphere, then there trivially holds

$$\delta(x) \geq \delta_{i_1}(x) = \|x - p(x)\| = \text{dist}(x, \partial\Omega^M). \quad (8.2)$$

Otherwise, define $\mathbf{m}_i = \{m_{i_1}, \dots, m_{i_r}\}$, i.e., the set of the centers of all spheres that contain y , and introduce the generalized cone

$$\text{cone}_y(\mathbf{m}_i) := \left\{ w = y + \sum_{t=1}^r \lambda_t v_t \mid 0 \leq \lambda_t \right\}, \quad v_t := \frac{m_{i_t} - y}{\|m_{i_t} - y\|}.$$

Then, following [9][Theorem 1], there holds that $x \in \text{cone}_y(\mathbf{m}_i)$. We now show that we can cover $\text{cone}_y(\mathbf{m}_i)$ with r circular cones with equal aperture. Indeed, considering the vector $-n(y)$ from Assumption **(A4)** we have

$$-n(y) \cdot v_t > \gamma_\alpha^\infty = \cos\left(\frac{\pi}{2} - \beta^\infty\right) = \cos(\alpha), \quad \forall t = 1, \dots, r.$$

Elementary geometrical considerations then yield that we can cover $\text{cone}_y(\mathbf{m}_i)$ with circular cones $K_y(v_t, \alpha)$, $t = 1, \dots, r$, of angle α , i.e.,

$$\text{cone}_y(\mathbf{m}_i) \subset \bigcup_{t=1}^r K_y(v_t, \alpha),$$

see Figure 8.1 (right) for an elementary illustration. Thus there exists a $j = i_s$, such that $x \in K_y(v_s, \alpha)$ holds. Then, choose the maximal radius $R_{j,\alpha} = R_j \sin(\alpha) > 0$ such that $B(m_j; R_{j,\alpha})$ is entirely contained in the circular cone $K_y(v_s, \alpha)$; see Figure 8.1 for a graphical illustration of the geometric situation. Due to $x \in \Omega_\varepsilon$ we have $\delta_j(x) \leq \delta(x) < \varepsilon$. First, this implies that

$$R_j - \|x - m_j\| < \varepsilon = R_{\min}^\infty(1 - \sin(\alpha)) \leq R_j(1 - \sin(\alpha)),$$

and $\|x - m_j\| > R_j \sin(\alpha) = R_{j,\alpha}$. From this we conclude

$$x \in K_y(v_j, \alpha) \cap \left(B(m_j; R_j) \setminus \overline{B(m_j; R_{j,\alpha})} \right).$$

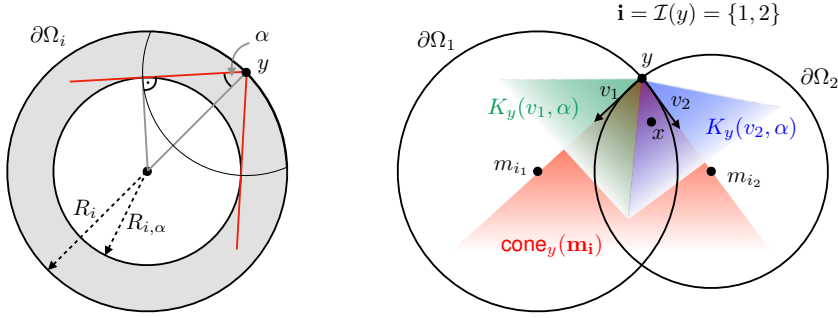


FIG. 8.1. Illustration on choosing the maximal radius $R_{i,\alpha}$ (left) and how to cover $\text{cone}_y(\mathbf{m}_i)$ with circular cones $K_y(v_t, \alpha)$ (right).

Second, if $\|x - y\| \leq R_{\min}^\infty \sin(\beta^\infty) = R_{\min}^\infty \cos(\alpha)$, then $x \in \overline{B(y; R_j \cos(\alpha))}$ and Lemma 8.1 (below) then states that

$$\delta_j(x) \geq \frac{\cos(\alpha)}{2} \text{dist}(x, \partial\Omega^M). \quad (8.3)$$

In consequence, equation (8.3) yields that

$$\frac{\cos(\alpha)}{2} \text{dist}(x, \partial\Omega^M) = \frac{\cos(\alpha)}{2} \text{dist}(x, y) \leq \delta_j(x) \leq \delta(x).$$

In the contrary case, i.e. if $\|x - y\| > R_{\min}^\infty \sin(\beta^\infty)$, then

$$\text{dist}(x, \partial\Omega^M) \leq 2R_j \leq 2R_{\max}^\infty \leq \frac{2R_{\max}^\infty}{\gamma_{\text{int}}} \delta(x),$$

by (3.5). Finally, define (cf. also (8.1), (8.2))

$$\gamma_b = \min \left\{ 1, \frac{R_{\min}^\infty (1 - \sin(\alpha))}{2R_{\max}^\infty}, \frac{\cos(\alpha)}{2}, \frac{\gamma_{\text{int}}}{2R_{\max}^\infty} \right\}, \quad (8.4)$$

and we obtain $\delta(x) \geq \gamma_b \text{dist}(x, \partial\Omega^M)$. \square

LEMMA 8.1. For $y \in \partial\Omega_i$ define $v_i := \frac{m_i - y}{\|m_i - y\|}$. For given $0 < \alpha < \frac{\pi}{2}$, consider the circular cone $K_y(v_i, \alpha)$ and let $R_{i,\alpha} > 0$ be the minimal radius such that $B(m_i; R_{i,\alpha})$ intersects the boundary $\partial K_y(v_i, \alpha)$, i.e. the maximal radius such that $B(m_i; R_{i,\alpha})$ is contained in the circular cone $K_y(v_i, \alpha)$. Then, the maximal value is given by $R_{i,\alpha} = R_i \sin(\alpha)$ and the following holds:

$$\delta_i(x) \geq c_\alpha \text{dist}(x, y), \quad \forall x \in K_y(v_i, \alpha) \cap (B(m_i; R_i) \setminus \overline{B(m_i; R_{i,\alpha})}) \cap \overline{B(y; R_i \cos(\alpha))}, \quad (8.5)$$

where $c_\alpha = \frac{\cos(\alpha)}{2} > 0$.

Proof. We consider any point $x \in \mathcal{P} = K_y(v_i, \alpha) \cap (B(m_i; R_i) \setminus \overline{B(m_i; R_{i,\alpha})}) \cap \overline{B(y; R_i \cos(\alpha))}$. Consider now all points in \mathcal{P} lying on a subset $\Gamma(x)$ of the sphere with radius $R_i - \delta_i(x)$:

$$\Gamma(x) = \{z \in \mathcal{P} \mid \delta_i(z) = \delta_i(x)\},$$

and introduce $d_i(x) = \max_{z \in \Gamma(x)} \text{dist}(z, y)$ such that $\delta_i(x) \leq \text{dist}(x, y) \leq d_i(x)$, and thus $\frac{\text{dist}(x, y)}{\delta_i(x)} \leq \frac{d_i(x)}{\delta_i(x)}$. Applying the cosine rule yields $(R_i - \delta_i(x))^2 = d_i(x)^2 + R_i^2 - 2d_i(x)R_i \cos(\alpha)$, which is equivalent to

$$\frac{d_i(x)}{\delta_i(x)} = \frac{2R_i - \delta_i(x)}{2R_i \cos(\alpha) - d_i(x)}.$$

Since $d_i(x) \leq d_i = R_i \cos(\alpha)$, we have

$$\frac{\delta_i(x)}{\text{dist}(x, y)} \geq \frac{\delta_i(x)}{d_i(x)} = \frac{2R_i \cos(\alpha) - d_i(x)}{2R_i - \delta_i(x)} \geq \frac{R_i \cos(\alpha)}{2R_i - \delta_i(x)} \geq \frac{\cos(\alpha)}{2},$$

which completes the proof. \square

8.2. Derivation of result in Remark 3.4. We consider the case of two overlapping balls, $\Omega^2 = \Omega_1 \cap \Omega_2$, with $\Omega_1 = B((-1, 0, 0); 2)$, $\Omega_2 = B((1, 0, 0); 2)$ as in Remark 3.4. The intersection of $\partial\Omega^2$ with $\Omega_1 \cap \Omega_2$ is given by the circle $S = \{(0, x_2, x_3) \mid x_2^2 + x_3^2 = 3\}$. We analyze the smoothness of θ_1 (close to S). Elementary computation yields

$$\nabla\theta_1 = \frac{\delta_2 \nabla\delta_1 - \delta_1 \nabla\delta_2}{\delta^2}, \quad \nabla\theta_1 \cdot \nabla\theta_1 = \frac{\delta_1^2 + \delta_2^2 - 2\delta_1\delta_2 \nabla\delta_1 \cdot \nabla\delta_2}{\delta^4}.$$

On the subdomain $V := \{x \in \Omega_1 \cap \Omega_2 \mid |x_1| \leq \frac{1}{2}, 1 \leq x_2^2 + x_3^2 \leq 3\}$ we have $|\nabla\delta_1 \cdot \nabla\delta_2| \leq \frac{3}{4}$. Hence,

$$(\nabla\theta_1 \cdot \nabla\theta_1)|_V \geq \frac{\delta_1^2 + \delta_2^2 - 1\frac{1}{2}\delta_1\delta_2}{\delta^4} \geq \frac{1}{4} \frac{\delta_1^2 + \delta_2^2}{\delta^4} \geq \frac{1}{8} \frac{1}{\delta^2}.$$

Take p on the intersection circle S and define the triangle T_p with the vertices p , $(-1, 0, 0)$, $(0, 0, 0)$. For all $x \in T_p$ we have $\delta_2(x) \leq \delta_1(x)$, hence $\delta(x) \leq 2\delta_1(x)$. Furthermore, there exists a constant c such that $\delta_1(x) \leq c\|x - p\|$ for all $x \in T_p \cap V$. The spherical sector obtained by rotating T_p along $p \in S$ can be parametrized by coordinates (s, ρ, θ) , with $s \in [0, 2\sqrt{3}\pi]$ the arclength parameter on S and (ρ, θ) polar coordinates in the triangle T_p at $p = s$, with origin at p . Integration over a part $T_S := \{(s, \rho, \theta) \mid \rho \leq \rho_0\}$ of this spherical sector, with $\rho_0 > 0$ sufficiently small, yields

$$\int_{T_S} |\nabla\theta_1|^2 dx \geq \frac{1}{16} \int_{T_S} \delta_1^{-2} dx \geq \tilde{c} \int_0^{2\sqrt{3}\pi} \int_0^{\frac{1}{6}\pi} \int_0^{\rho_0} \frac{1}{\rho^2} \rho d\rho d\theta ds = \infty.$$

REFERENCES

- [1] ERIC CANCÈS, YVON MADAY, AND BENJAMIN STAMM, *Domain decomposition for implicit solution models*, The Journal of Chemical Physics, 139 (2013), p. 054111.
- [2] FAYÇAL CHAOUQUI, GABRIELE CIARAMELLA, MARTIN J GANDER, AND TOMMASO VANZAN, *On the scalability of classical one-level domain-decomposition methods*, Vietnam Journal of Mathematics, 46 (2018), pp. 1053–1088.
- [3] GABRIELE CIARAMELLA AND MARTIN J GANDER, *Analysis of the parallel Schwarz method for growing chains of fixed-sized subdomains: Part I*, SIAM Journal on Numerical Analysis, 55 (2017), pp. 1330–1356.
- [4] ———, *Analysis of the parallel Schwarz method for growing chains of fixed-sized subdomains: Part II*, SIAM Journal on Numerical Analysis, 56 (2018), pp. 1498–1524.
- [5] ———, *Analysis of the parallel Schwarz method for growing chains of fixed-sized subdomains: Part III*, Electronic Transactions on Numerical Analysis, 49 (2018), pp. 210–243.

- [6] GABRIELE CIARAMELLA, MUHAMMAD HASSAN, AND BENJAMIN STAMM, *On the scalability of the Schwarz method*, The SMAI journal of computational mathematics, 6 (2020), pp. 33–68.
- [7] MICHAEL L CONNOLLY, *Analytical molecular surface calculation*, Journal of applied crystallography, 16 (1983), pp. 548–558.
- [8] V. DOLEAN, P. JOLIVET, AND F. NATAF, *An Introduction to Domain Decomposition Methods: Algorithms, Theory and Implementation*, SIAM, 2015.
- [9] XIANGLONG DUAN, CHAOYU QUAN, AND BENJAMIN STAMM, *A boundary-partition-based voronoi diagram of d-dimensional balls: definition, properties, and applications*, Adv Comput Math, 46 (2020), p. 44.
- [10] D. GILBARG AND N.S. TRUDINGER, *Elliptic Partial Differential Equations of Second Order*, Springer, 1977.
- [11] P. HAJLASZ, *Pointwise Hardy inequalities*, Proc. American Math. Soc., 127 (1999), pp. 417–423.
- [12] L.I. HEDBERG, *On certain convolution inequalities*, Proc. American Math. Soc., 36 (1972), pp. 505–510.
- [13] J. KINNUNEN AND O. MARTIO, *Hardy’s inequalities for Sobolev functions*, Math. Research Letters, 4 (1997), pp. 489–500.
- [14] A. KLAMT AND G. SCHÜÜRMMANN, *COSMO: a new approach to dielectric screening in solvents with explicit expressions for the screening energy and its gradient*, J. Chem. Soc., Perkin Trans. 2, (1993), pp. 799–805.
- [15] BYUNGKOOK LEE AND FREDERIC M RICHARDS, *The interpretation of protein structures: estimation of static accessibility*, Journal of molecular biology, 55 (1971), pp. 379–IN4.
- [16] FILIPPO LIPPARINI, LOUIS LAGARDÈRE, GIOVANNI SCALMANI, BENJAMIN STAMM, ERIC CANCÈS, YVON MADAY, JEAN-PHILIP PIQUEMAL, MICHAEL J FRISCH, AND BENEDETTA MENNUCCI, *Quantum calculations in solution for large to very large molecules: A new linear scaling QM/continuum approach*, The journal of physical chemistry letters, 5 (2014), pp. 953–958.
- [17] FILIPPO LIPPARINI AND BENEDETTA MENNUCCI, *Perspective: Polarizable continuum models for quantum-mechanical descriptions*, The Journal of chemical physics, 144 (2016), p. 160901.
- [18] FILIPPO LIPPARINI, GIOVANNI SCALMANI, LOUIS LAGARDÈRE, BENJAMIN STAMM, ERIC CANCÈS, YVON MADAY, JEAN-PHILIP PIQUEMAL, MICHAEL J FRISCH, AND BENEDETTA MENNUCCI, *Quantum, classical, and hybrid QM/MM calculations in solution: General implementation of the ddCOSMO linear scaling strategy*, The Journal of Chemical Physics, 141 (2014), p. 184108.
- [19] FILIPPO LIPPARINI, BENJAMIN STAMM, ERIC CANCÈS, YVON MADAY, AND BENEDETTA MENNUCCI, *Fast domain decomposition algorithm for continuum solvation models: Energy and first derivatives*, Journal of Chemical Theory and Computation, 9 (2013), pp. 3637–3648.
- [20] CH. QUAN AND B. STAMM, *Mathematical analysis and calculation of molecular surfaces*, J. Comp. Phys., 322 (2016), pp. 760–782.
- [21] FREDERIC M. RICHARDS, *Areas, volumes, packing, and protein structure*, Annual Review of Biophysics and Bioengineering, 6 (1977), pp. 151–176.
- [22] BENJAMIN STAMM, LOUIS LAGARDÈRE, GIOVANNI SCALMANI, PAOLO GATTO, ERIC CANCÈS, JEAN-PHILIP PIQUEMAL, YVON MADAY, BENEDETTA MENNUCCI, AND FILIPPO LIPPARINI, *How to make continuum solvation incredibly fast in a few simple steps: a practical guide to the domain decomposition paradigm for the conductor-like screening model continuum solvation, linear scaling, domain decomposition*, International Journal of Quantum Chemistry, (2018).
- [23] E.M. STEIN, *Singular Integrals and Differentiability Properties of Functions*, Princeton University Press, 1970.
- [24] JACOPO TOMASI, BENEDETTA MENNUCCI, AND ROBERTO CAMMI, *Quantum mechanical continuum solvation models*, Chemical reviews, 105 (2005), pp. 2999–3094.
- [25] A. TOSELLI AND O. WIDLUND, *Domain Decomposition Methods - Algorithms and Theory*, Springer, 2004.
- [26] J. XU, *Iterative methods by space decomposition and subspace correction*, SIAM Review, 34 (1992), pp. 581–613.
- [27] J. XU AND L. ZIKATANOV, *The method of alternating projections and the method of subspace corrections in Hilbert space*, J. of the American Mathematical Society, 15 (2002), pp. 573–597.
- [28] W. ZHENG AND H. QI, *On Friedrichs-Poincaré-type inequalities*, J. Math. Anal. Appl., 304 (2005), pp. 542–551.
- [29] W. ZIEMER, *Weakly Differentiable Functions*, Springer, 1989.